LOCKHEED MARTIN ENERGY RESEARCH LIBRARIES

3 4456 0444873 8

ORNL/TM-13605

OAK RIDGE NATIONAL LABORATORY

LOCKHEED MARTIN

Hydrogen Detonation Study for Cold Source Design of High Flux Isotope Reactor

S. H. Kim
R. P. Taleyarkhan
D. Cook
C. Hyman
A. T. Lucas

OAK RIDGE NATIONAL LABORATORY
CENTRAL RESEARCH LIBRARY
CIRCULATION SECTION
4500N ROOM 175
LIBRARY LOAN COPY
DO NOT TRANSFER TO ANOTHER PERSON
If you wish someone else to see this report, send in name with report and the library will arrange a loan.
ORNL-1813 (6-97)

MANAGED AND OPERATED BY
LOCKHEED MARTIN ENERGY RESEARCH CORPORATION
FOR THE UNITED STATES
DEPARTMENT OF ENERGY

ORNL-27 (9-96)

This report has been reproduced directly from the best available copy.

Available to DOE and DOE contractors from the Office of Scientific and Technical Information, P.O. Box 62, Oak Ridge, TN 37831; prices available from (615) 576-8401, FTS 626-8401.

Available to the public from the National Technical Information Service, U.S. Department of Commerce, 5285 Port Royal Rd., Springfield, VA 22161.

This report was prepared as an account of work sponsored by an agency of the United States Government. Neither the United States Government nor any agency thereof, nor any of their employees, makes any warranty, express or implied, or assumes any legal liability or responsibility for the accuracy, completeness, or usefulness of any information, apparatus, product, or process disclosed, or represents that its use would not infringe privately owned rights. Reference herein to any specific commercial product, process, or service by trade name, trademark, manufacturer, or otherwise, does not necessarily constitute or imply its endorsement, recommendation, or favoring by the United States Government or any agency thereof. The views and opinions of authors expressed herein do not necessarily state or reflect those of the United States Government or any agency thereof.

ORNL/TM-13605

Hydrogen Detonation Study for Cold Source Design of High Flux Isotope Reactor

S. H. Kim
R. P. Taleyarkhan
D. Cook
C. Hyman
A. T. Lucas

April, 1998

Prepared by the
Oak Ridge National Laboratory
Oak Ridge, Tennessee 37831-8045
managed by
LOCKHEED MARTIN ENERGY SYSTEMS, INC.
for the
U.S. DEPARTMENT OF ENERGY
under contract DOE-840R21400

LOCKHEED MARTIN ENERGY RESEARCH LIBRARIES

3 4456 0444873 8

ACKNOWLEDGMENTS

The authors wish to acknowledge the significant technical interactions with HFIR technical and management staff. Trevor Lucas provided key insights on structural geometry and damage states of interest. Feedback provided by J. Freels was useful in guiding the various calculations reported in this document. S. Chang provided insights on structural response issues and loading function needs for conduct of follow-on structural assessments. Finally, the financial support provided by Doug Selby is gratefully acknowledged.

TABLE OF CONTENTS

		PAGE
Acknowledgements		ii
Table of Contents		iii
List of Tables		iv
List of Figures		v
Abstract		1
1	INTRODUCTION	2
2	FRONT-END EVALUATION OF DETONATION PROCESS	4
3	EVALUATION OF DYNAMIC DETONATION PROCESS	7
	3.1 Case 1 Results: Detonation at (0,0)	8
	3.2 Case 2 Results: Detonation at (0, -10)	9
	3.3 Case 3 Results - Multiple Volumetric Detonations	10
	3.4 One-Dimensional Simulation of Case 1	10
4	SUMMARY AND CONCLUSION	11
5	REFERENCES	12

LIST OF TABLES

PAGE

Table 1 Detonation Parameters Estimated Using CET89 and Analytical Calculations 5

LIST OF FIGURES

PAGE

Figure 1 Schematic Representation of Proposed HFIR Cold Source.....6

Figure 2 Chapman-Jouguet Detonation Pressure and Temperature as a Function of Initial Temperature for Variable Air/Hydrogen Mixtures.....6

Figure 3 Detonation Velocity as a Function of Initial Temperature for Variable Air/Hydrogen Mixtures 7

Figure 4 Vacuum Tube Modeled for CTH Calculations With Tracer Points 13

Figure 5(a) Pressure Profile Along y=0 line from 0 to 21μsec With 3μsec Time Interval for Case 1 14

Figure 5(b) Pressure Profile Along y=0 line from 23 to 47μsec Time Interval for Case 1 14

Figure 5(c) Pressure Profile Along y=0 line from 49 to 79μsec Time Interval for Case 1 15

Figure 6(a) Pressure Profile Along r=0 line from 0 to 21μsec Time Interval for Case 1 15

Figure 6(b) Pressure Profile Along r=0 line from 22 to 53μsec with 3μsec Time Interval for Case 1 16

Figure 6(c) Pressure Profile Along r=0 line from 54 to 101μsec with 3μsec Time Interval for Case 1 16

Figure 7(a) Pressure Profile Along y=21 line from 80 to 101μsec with 84μsec Time Interval for Case 1 17

Figure 7(b) Pressure Profile Along y=21 line from 85 to 103μsec with 2μsec Time Interval for Case 1 17

Figure 7(c) Pressure Profile Along y=-21 line from 104 to 129μsec with 3μsec Time Interval for Case 1 18

Figure 8(a) Pressure History in Hydrogen/Air Mixture Near the Vacuum Tube Wall of Case 1 18

Figure 8(b) Pressure History in Hydrogen/Air Mixture Near the Vacuum Tube Wall of Case 1 19

LIST OF FIGURES (CONTINUED)

PAGE

Figure 8(c) Pressure History in Hydrogen/Air Mixture Near the Vacuum Tube Wall of Case 1 19

Figure 8(d) Pressure History in Hydrogen/Air Mixture Near the Vacuum Tube Wall of Case 1 20

Figure 9 Pressure History in Hydrogen/Air Mixture Along r=0 of Case 1....20

Figure 10(a) Temperature in Hydrogen/Air Mixture Near the Vacuum Tube Wall of Case 1 21

Figure 10(b) Temperature in Hydrogen/Air Mixture Near the Vacuum Tube Wall of Case 1 21

Figure 10(c) Temperature in Hydrogen/Air Mixture Near the Vacuum Tube Wall of Case 1 22

Figure 10(d) Temperature in Hydrogen/Air Mixture Near the Vacuum Tube Wall of Case 1 22

Figure 11 Temperature in Hydrogen/Air Mixture Along r=0 of Case 1....23

Figure 12(a) Pressure Profile Along r=0 line from 0 to 51μsec with 3μsec Time Interval for Case 2 23

Figure 12(b) Pressure Profile Along r=0 line from 52 to 61μsec with 2μsec Time Interval for Case 2 24

Figure 12(c) Pressure Profile Along r=0 line from 62 to 76μsec with 1μsec Time Interval for Case 2 24

Figure 12(d) Pressure Profile Along r=0 line from 77 to 93μsec with 1μsec Time Interval for Case 2 25

Figure 13(a) Pressure Profile Along y=-21 line from 42 to 48μsec with 1μsec Time Interval for Case 2 25

Figure 13(b) Pressure Profile Along y=-21 line from 49 to 73μsec with 3μsec Time Interval for Case 2 26

Figure 13(c) Pressure Profile Along y=-21 line from 74 to 100μsec with 3μsec Time Interval for Case 2 26

LIST OF FIGURES (CONTINUED)

PAGE

Figure 13(d) Pressure Profile Along y=-21 line from 101 to 133μsec with 3μsec Time Interval for Case 2 27

Figure 14(a) Pressure History in Hydrogen/Air Mixture Near the Vacuum Tube Wall of Case 2 27

Figure 14(b) Pressure History in Hydrogen/Air Mixture Near the Vacuum Tube Wall of Case 2 28

Figure 14(c) Pressure History in Hydrogen/Air Mixture Near the Vacuum Tube Wall of Case 2 28

Figure 14(d) Pressure History in Hydrogen/Air Mixture Near the Vacuum Tube Wall of Case 2 29

Figure 15 Pressure History in Hydrogen/Air Mixture Along r=0 of Case 2 29

Figure 16(a) Temperature in Hydrogen/Air Mixture Near the Vacuum Tube Wall of Case 2 30

Figure 16(b) Temperature in Hydrogen/Air Mixture Near the Vacuum Tube Wall of Case 2 30

Figure 16(c) Temperature in Hydrogen/Air Mixture Near the Vacuum Tube Wall of Case 2 31

Figure 16(d) Temperature in Hydrogen/Air Mixture Near the Vacuum Tube Wall of Case 2 31

Figure 17 Temperature History in Hydrogen/Air Mixture Along r=0 of Case 2 ..32

Figure 18(a) Pressure Profile Along r=0 line from 0 to 18μsec with 3μsec Time Interval for Case 3 32

Figure 18(b) Pressure Profile Along r=0 line from 19 to 22μsec with 1μsec Time Interval for Case 3 33

Figure 18(c) Pressure Profile Along r=0 line from 23 to 39μsec with 3μsec Time Interval for Case 3 33

Figure 18(d) Pressure Profile Along r=0 line from 40 to 46μsec with 1μsec Time Interval for Case 3 34

Figure 18(e) Pressure Profile Along r=0 line from 47 to 70μsec with 3μsec Time Interval for Case 3 34

LIST OF FIGURES (CONTINUED)

PAGE

Figure 18(f) Pressure Profile Along r=0 line from 71 to 86μsec with 3μsec Time Interval for Case 3 35

Figure 18(g) Pressure Profile Along r=0 line from 87 to 119μsec with 3μsec Time Interval for Case 3 35

Figure 19(a) Pressure History in Hydrogen/Air Mixture Near the Vacuum Tube Wall of Case 3 36

Figure 19(b) Pressure History in Hydrogen/Air Mixture Near the Vacuum Tube Wall of Case 3 36

Figure 19(c) Pressure History in Hydrogen/Air Mixture Near the Vacuum Tube Wall of Case 3 37

Figure 19(d) Pressure History in Hydrogen/Air Mixture Near the Vacuum Tube Wall of Case 3 37

Figure 20 Pressure History in Hydrogen/Air Mixture Along r=0 of Case 3 38

Figure 21(a) Temperature in Hydrogen/Air Mixture Near the Vacuum Tube Wall of Case 3 38

Figure 21(b) Temperature in Hydrogen/Air Mixture Near the Vacuum Tube Wall of Case 3 39

Figure 21(c) Temperature in Hydrogen/Air Mixture Near the Vacuum Tube Wall of Case 3 39

Figure 21(d) Temperature in Hydrogen/Air Mixture Near the Vacuum Tube Wall of Case 3 40

Figure 22 Temperature History in Hydrogen/Air Mixture Along r=0 of Case 3 ..40

Figure 23 Tracer Points Modeled in 1-D Simulations of Case 1 41

Figure 24(a) Pressure History in Hydrogen/Air Mixture of 1-D Simulations.....41

Figure 24(b) Pressure History in Hydrogen/Air Mixture of 1-D Simulations.....42

Figure 24(c) Pressure History in Hydrogen/Air Mixture of 1-D Simulations.....42

Figure 24(d) Pressure History in Hydrogen/Air Mixture of 1-D Simulations.....43

Abstract

The High-Flux Isotope Reactor (HFIR) is a 85-MW research reactor located at the Oak Ridge National Laboratory (ORNL). Several beam tubes penetrate through the reflector, one of which is to include a cold source. The HFIR cold source is to utilize supercritical hydrogen as a moderator for production of cold neutrons. Significant efforts have been introduced in the design effort to keep the likelihood of hydrogen-air detonations within the vacuum tube region to an extremely low value ($< 10^{-6}$/y). A study was initiated to evaluate the consequences of a hydrogen detonation and to demonstrate system robustness. This report presents a perspective overview of the modeling work as well as results of hydrogen detonation assessments for evaluating the safety margins associated with hydrogen detonation events in the proposed cold source of the HFIR. Three cases of different detonation locations were assumed for same initial conditions of 92K, and 0.1MPa for a stoichiometric air/hydrogen mixture. Cases 1 and 2 assume a point detonation initiated at different locations, while case 3 simulates volumetric detonation with multiple simultaneous detonation points. Also, a 1-D calculation was made for a case similar to case 1. When the detonation initiates at the center of the hemispherical cap of the vacuum tube as in case 1, the maximum pressure imposed onto the wall was estimated at ~12.5MPa near the nose tip portion of the vacuum tube cap. The other cases show that at the same location, the maximum pressure loading can be as high as ~30MPa. As the initial detonation point moves away from the point assumed for case 1, the maximum pressure in the gas mixture occurs closer to the wall near the nose tip of the vacuum tube cap. The secondary wave from case 2 is seen to be ~25MPa when it moves out of the system boundary, whereas for case 1 ~15MPa is obtained. High temperatures of the gas mixture is another concern. The gas temperature near the structure wall remains at ~3000K for a significant period of time. Inner surface of the tube wall will be heated to a high temperature while outer wall remains cold. Thermal stress due to such a large temperature difference across the wall needs to be assessed.

1. Introduction

The High-Flux Isotope Reactor (HFIR) is a 85-MW research reactor located at the Oak Ridge National Laboratory (ORNL). The reactor core is surrounded with a beryllium reflector. Several beam tubes penetrate through the reflector, one of which is to include a cold source (as part of an effort to upgrade HFIR's capabilities). The HFIR cold source is to utilize supercritical hydrogen as a moderator for production of cold neutrons. Significant efforts have been introduced in the design effort to keep the likelihood of hydrogen-air detonations within the vacuum tube region to an extremely low value ($< 10^{-6}$/y) to ensure that overall risk of such hypothetical events is acceptable.

A defense-in-depth philosophy has been adopted by HFIR designers and management. Therefore, despite the low initiating event frequencies associated with detonation events, a study was initiated to evaluate the consequences of a hydrogen detonation and to demonstrate system robustness. This report presents a perspective overview of the modeling work as well as results of hydrogen detonation assessments for evaluating the safety margins associated with hydrogen detonation events in the proposed cold source of the HFIR.

A schematic representation of the pertinent HFIR cold-source structures is depicted in Figure 1. As seen, it consists of a moderator vessel enclosed in a vacuum tube, which is further surrounded by several other structural members (including a water gap, etc.). A series of conservative assumptions were made to attain a state wherein air in-leakage takes place within the vacuum tube volume located within the beryllium reflector. These assumptions led to an initial state (gas mixture temperature of ~90 K at 0. 1MPa) wherein approximately 90g of hydrogen-nitrogen-oxygen mixture fills a space of about 23L in volume.

The problem to be solved consists of determining the dynamic temperatures, pressures and stress states associated with a hydrogen detonation event within the vacuum tube. The scenario to be resolved is one wherein it is assumed that a mixture of hydrogen and air fills the entire vacuum tube volume and then detonates due to spontaneously-occurring initiators (e.g., electrostatics), thereby, avoiding needless arguments related to absence or presence of such initiators. For evaluation of structural response a detonation wave is to be modeled as initiating at set locations and then allowed to propagate outwards spherically. In order to bound the actual location of initiating locations, it was decided to model the onset of detonation at various discrete locations as well as assuming volumetric detonation (viz., to

model effects of distributed sparks). Finally, it was assumed that a two-dimensional (2-D) symmetric simulation of the shock wave generation, its transport and interactions with surrounding structures is adequate for capturing the principal effects of a detonation event in the HFIR cold source vacuum tube.

The principal tools being used for evaluations are the CET89 and CTH computer codes. CET89 is a chemical equilibrium code developed to calculate thermodynamic and transport properties of complex chemical systems [1]. CTH is a highly sophisticated tool to be developed to model shock wave physics, fluid-structure interactions, missile penetration dynamics, together with multimaterial motion and response in one, two and three dimensions [2]. It has been utilized in the past for analyzing hydrogen detonation events in power reactor and research reactor containment [3-5]. For the best-estimate evaluation of hydrogen detonation studies, CET89 was first used to evaluate detonation parameters results (for a Chapman-Jouguet or C-J detonation*) such as post-burn mixture density, specific heat ratio of pre- and post-burn mixture, detonation velocity, shock burn energy, etc. It also provides estimates of static pressure and temperature increase after the burn completes. These CET89 evaluations set the stage for appropriate CTH model input for simulating a high explosive burning process. Thereafter, CTH can be used (as has been done in the past) for evaluating important effects related to fluid-structure interactions as well as to capture possible effects of wave focusing.

---

* Regardless of the nature of the combustion process, i.e., detonation or simple deflagration, a final equilibrium pressure will be reached. The standard model used for calculating the equilibrium pressure is the Adiabatic, Isochoric, Complete Combustion (AICC) model and the final equilibrium pressure is termed the AICC pressure. The AICC model assumptions result in the highest possible "equilibrium" pressures. Heat transfer, volume expansion, and incomplete combustion will result in a lower pressure. If the AICC process assumptions are met, then at equilibrium, simple deflagrations, accelerated flames and detonations reach the same final AICC pressure. The difference between detonations and deflagrations in a confined volume is the transient pressure time-histories between ignition and final equilibrium. The pressure of a freely propagating detonation significantly exceeds the equilibrium AICC pressure. Such a peak detonation pressure is given by the Chapman-Jouguet (C-J) model. The C-J model is derived from conservation of mass, momentum and energy across a one-dimensional flow discontinuity. The C-J model predicts the thermodynamic state immediately behind the detonation wave. Assuming that the ratio of specific heat, γ, is the same for reactants and products, a simple relationship between the CJ and AICC pressures can be approximated as [6]

$$\frac{P_{CJ}}{P_o} = 2\left(\frac{P_{AICC}}{P_o}\right) - \frac{1}{1+\gamma}$$

Gaseous detonation can be modeled in CTH by specifying the appropriate gas mixture as a "high explosive." The high explosive detonation option in CTH uses a programmed burn model. In this model a burn is simulated by the release of internal energy in a small region (two or three computational cells) which moves through the mesh at a constant detonation velocity that is specified by the user as an input parameter along with some other detonation parameters. The energy release corresponds to the chemical energy released in a detonation. The location and time of ignition must also be specified by the user. In this report, we present front-end evaluations of the detonation process using the CET89 code, along with detonation wave propagation, its interaction with structures and dissipation using the CTH code.

2. Front-end Evaluation of Detonation Process

The CET89 code was utilized for conducting parametric studies in a lumped framework to evaluate levels of possible pressurization, detonation velocities, temperatures of burn mixtures, etc. This work was conducted for three different concentrations ranging from the lower detonation limit of 12 vol.% to the upper limit of 58 vol.% of hydrogen including the stoichiometric value of ~29 vol.%.

As may be expected, several uncertainties exist related to the initial state of the mixture, the key variables being the thermal environment, and the hydrogen concentration. In order to bound these uncertainties CET89 code calculations were conducted over a range of these key parameters (from a baseline system pressure of 0.1 MPa). Results of these evaluations with CET89 are plotted graphically in Figures 2 and 3 for various initial system temperatures, and at the three different hydrogen concentrations of 12, 29 and 58 vol.% respectively.

The results shown in Figures 2 and 3 are noteworthy. It is clearly seen that temperature and hydrogen concentration play a predominant role in determining the ratios of pressure and temperature increases, and to a lesser extent the detonation velocity. At all temperatures, the concentration significantly impacts the detonation velocity. However, at the same concentration, the detonation velocity does not change much, but the initial temperature significantly impacts the ratio of pressure and temperature rise. As is clearly seen, at 92 K, the pressure rise ratio is about 50 (for 29 vol.%), whereas, the value drops to only 4 if the initial mixture temperature is 1000 K. This is understandable as the amount of chemical energy available for the 1000K case compared to the 92K case is rather limited assuming

the same value of initial pressure. For all cases, the values of pressure and temperature rise ratios are greatest, as might be expected, for stoichiometric mixtures of hydrogen and air. It is seen from these assessments that, at an initial temperature of 92 K, the detonation C-J pressure is likely to be a factor of about 50 larger than the initial system pressure. Therefore, the fully reflected pressure (in a 1-D framework) would tend to be about 100 times the initial system pressure. Per preliminary structural dynamics assessments, it is expected that this detonation gas pressures of about 10MPa will be possible to sustain in the HFIR cold source system at the moderator vessel location without unacceptable structural damage to the beam tube. Table 1 lists detonation parameters calculated using CET89 for various initial temperatures and mixture ratios. The same table also includes CET89 calculated C-J pressures to be compared against simple analytical calculations with various assumed values of specific heat ratio. These analytical calculations are based on constant specific heat and density of pre- and post-burn mixtures.

Table 1. Detonation Parameters Estimated Using CET89 and Analytical Calculations

										γ_{pre}	γ_{post}	γ_{avg}
Temp (K)	v %	P_{CJ}/P_o	T/T_o	γ_{pre}	γ_{post}	u	M	c_{pre}	c_{post}	P_{CJ}/P_o (calc)	P_{CJ}/P_o (calc)	P_{CJ}/P_o (calc)
92	12	32.29	19.77	1.39	1.27	1491	7.20	207	845	30.58	29.40	30.01
92	29	50.69	31.93	1.40	1.18	2000	8.83	227	1092	45.95	42.65	44.38
92	58	38.07	23.62	1.42	1.27	2214	7.75	286	1253	35.66	34.01	34.86
200	12	15.35	9.52	1.40	1.26	1502	4.91	306	863	14.47	13.88	14.19
200	29	23.26	14.68	1.40	1.17	1983	5.94	334	1091	21.00	19.47	20.27
200	58	17.98	11.28	1.41	1.26	2225	5.31	419	1273	16.88	16.15	16.53
293	12	10.75	6.75	1.40	1.26	1510	4.08	370	877	10.12	9.70	9.92
293	29	15.87	10.05	1.40	1.16	1971	4.88	404	1092	14.31	13.27	13.82
293	58	12.55	7.93	1.40	1.26	2234	4.41	506	1289	11.78	11.28	11.54
500	12	6.64	4.26	1.39	1.25	1525	3.17	481	906	6.25	6.01	6.13
500	29	9.30	5.95	1.39	1.16	1945	3.70	525	1098	8.39	7.82	8.12
500	58	7.69	4.94	1.39	1.24	2248	3.41	659	1321	7.19	6.89	7.05
750	12	4.68	3.08	1.36	1.23	1538	2.63	585	938	4.42	4.26	4.34
750	29	6.19	4.02	1.37	1.15	1915	3.00	638	1107	5.62	5.28	5.46
750	58	5.35	3.49	1.38	1.22	2254	2.81	803	1351	4.99	4.78	4.89
1000	12	3.69	2.47	1.34	1.21	1545	2.31	670	964	3.48	3.37	3.42
1000	29	4.63	3.05	1.35	1.14	1884	2.58	732	1118	4.23	4.01	4.13
1000	58	4.14	2.75	1.36	1.20	2247	2.44	921	1376	3.86	3.70	3.78

v% = hydrogen volume percent, u = detonation velocity,

c_{pre} = sonic velocity of preburn gas, c_{post} = sonic velocity of postburn gas, M = mach number

$\gamma_{pre} = c_p / c_v$, for preburn gas mixture, P_{CJ}/P_o (calc)= $1+[\gamma/(1+\gamma)]\ [M^2_{preburn} - 1]$

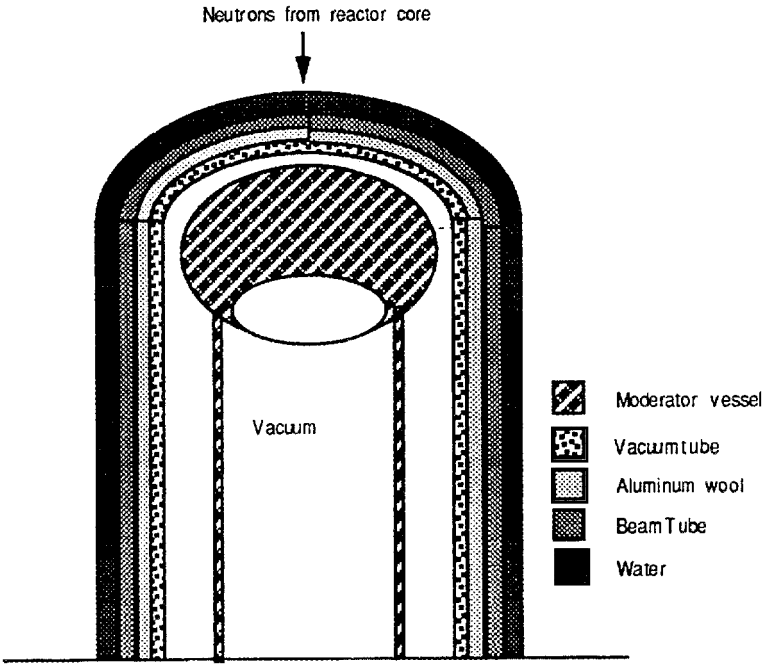

Figure 1. Schematic representation of proposed HFIR Cold Source

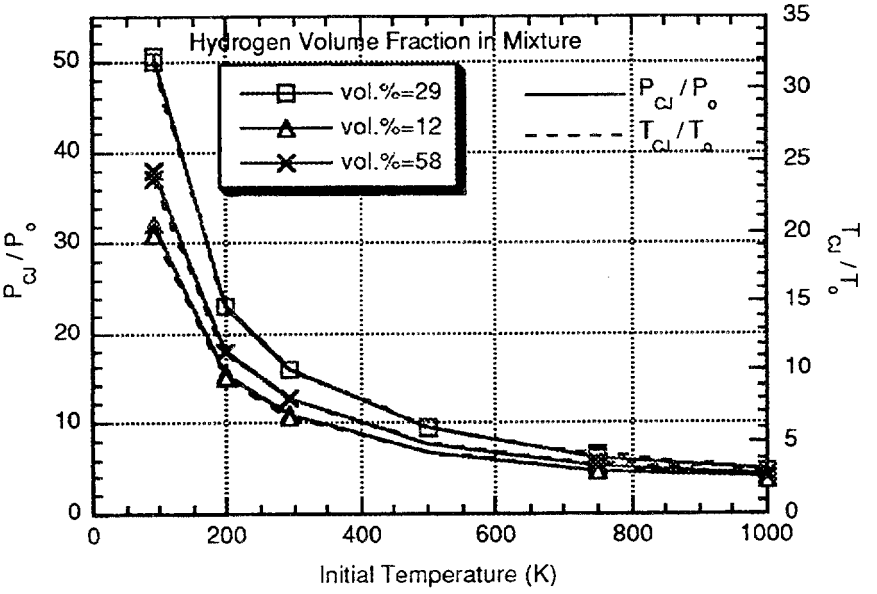

Figure 2. Chapman-Jouguet Detonation Pressure and Temperature as a function of Initial Temperature for Variable Air/Hydrogen Mixtures

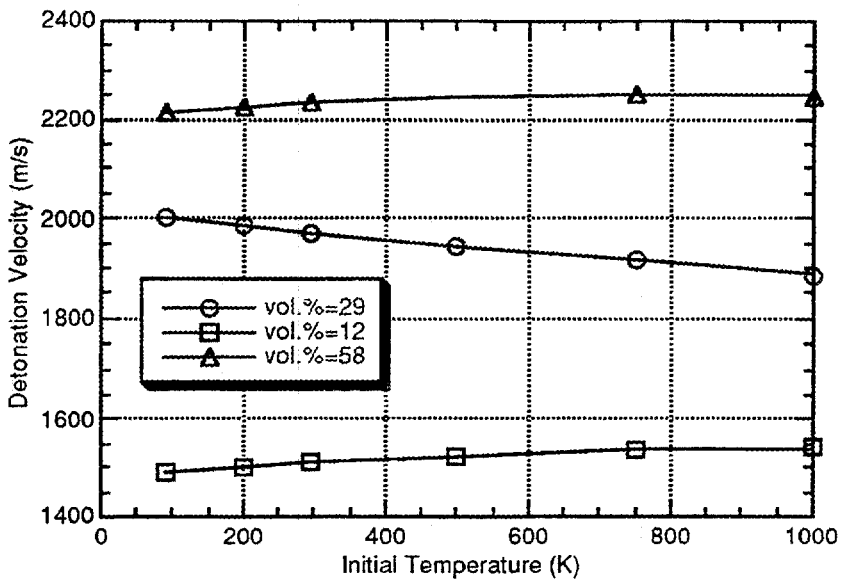

Figure 3. Detonation Velocity as a function of Initial Temperature for Variable Air/Hydrogen Mixtures

3. Evaluation of Dynamic Detonation Process

CET89 code calculations provide valuable information for first-cut assessments, but do not account for energy losses, thermal stresses or focusing effects of shock waves. CET89 results, however, provide the necessary detonation parameters (e.g., energy of detonation, burn mixture properties, detonation velocity for flame-front) for initializing CTH shock wave calculations. A two-dimensional cylindrical vacuum tube is modeled for CTH calculations as shown in Figure 4. Outside the vacuum tube is aluminum wool where helium gas flows through to detect vacuum leak. In this study of hydrogen detonation, it was assumed that the vacuum tube with uniform thickness (e.g., 0.32 cm) was surrounded by air and filled with uniform stoichiometric mixture (e.g., 29 vol.%) of air and hydrogen of 92K and 0.1MPa before detonation initiated. Pressure and temperature are monitored at tracer points depicted in Figure 4. The presence of internal structures inside the vacuum tube (as seen in Figure 1) is not modeled in the CTH analysis. The role of such structures (such as the moderator vessel and the transfer lines) on delivered loads is not clear. They may act to absorb combustion energy to mitigate the loading delivered to the internal hemispherical surface of the vacuum tube. However, the time scale for energy transfer/absorption is usually much longer to compare with that of shock transport and reaction with structures. Therefore, it is possible with the presence of these internal structures, that a shock can be amplified near the vacuum tube surface. It is unclear to

define the role of such internal structures until actual simulation to be conducted with inclusion of those internal structures.

Three cases of CTH calculations were performed. Case 1 assumes that a detonation was initiated at a point (r=0, and y=0) as seen in Figure 4. For Case 2, a point detonation was initiated at the location of r=0 and y=-10cm. Case 3 simulates volumetric detonation; that is a whole region of the vacuum tube volume are assumed to detonate simultaneously. In simulating volumetric detonation for case 3, multiple point detonations are assumed to be triggered at several locations (viz; at every ~2.5cm intervals) throughout the whole vacuum tube volume.

3.1 Case 1 Results : Detonation at (0,0)

The results for the case 1 are shown in Figures 5 through 11. Figures 5 - 7 show pressure wave propagation along a fixed line of a coordinate as shown in Figure 4 (i.e., r=0cm line, y=0cm line, y=-10cm line, etc.). Dotted lines in the figures indicate material boundaries; that is, the small region between two dotted lines represent vacuum tube wall structure. As seen in Figure 5, detonation initiated at the location (0,0) proceeds towards the vacuum tube wall. As the pressure is reflected at the wall as seen in Figure 5(b), its magnitude amplifies from ~6MPa to ~12MPa. However, when it travels back inwards, its amplification returns to the original pressure magnitude. One can notice that this reflected wave grows fast as it focuses near the location (0,0) to above 30MPa, which is shown in Figures 5(b) & (c). Figure 6 also shows the wave propagation along the r=0 line. As we already saw from Figure 5, the wave behaves in a similar manner such as reflection at the wall, focusing near the location (0,0) to above ~40MPa, and chasing down the original detonation wave. If we examine Figure 6(b) closely, we can find that the maximum wave focusing occurs at the location close to y=-2cm. The secondary (reflected) wave, as seen in Figure 6(c), becomes smaller as it moves away from the focused point and approaches the system boundary. By modeling the lower boundary as sound speed-based absorbing interface (representing a semi-infinite region), these waves along with a corresponding energy disappear as they reach this boundary (e.g., y=-21cm line). From the same figure, we can also notice that the rate of dissipation of the reflected wave as it approach to the y=-21cm boundary becomes close to constant. Therefore, when the reflected wave leaves the boundary, it is almost a constant value of ~15MPa. This value may be used as the magnitude of largest pressure wave hitting the vacuum tube window located at ~1.6m down away from this boundary. However, this pressure wave of 15MPa is a wave

focused near r=0 line. Figure 7 shows pressure wave distribution across the cross-section of the vacuum tube when it leaves the boundary, y=-21cm.

Figures 8 through 11 illustrate temporal variations of pressure and temperature at various locations. Each location is identified as a tracer point defined in Figure 4. Tracer points 1 through 13 indicate an air/hydrogen mixture region near the vacuum tube wall. The points 27 through 30 indicate the tracer points along the center line of the tube (i.e., r=0 line). It is seen from Figure 8, that the tracer point 1 experiences the highest pressure load, ~13MPa. Figure 9 shows the focused wave at the tracer point 27 is as large as ~30MPa. Figures 10 & 11 show the temperature variations at the same tracer points. Temperature as the mixture detonates, rises to ~3000K. At a certain location like the point 27 where the pressure wave is focused, the temperature is shown to increase to ~5500K as the gas mixture is compressed. During this time frame (lasting in ~140μsec), heat transfer to the wall is not great since it takes ~10 to ~100ms before the wall surface becomes significantly hot. This high temperature distribution along the wall may cause significant thermal stresses in the vacuum tube wall, and it has to be considered in the wall stress analysis.

3.2 Case 2 Results : Detonation at (0,-10)

For the case 2, the detonation was assumed to start at the location y=-10cm along the center line (r=0). Similar as in the case 1, results show the detonation wave propagation and amplification as the reflected wave is focused. Figure 12(b) shows that the reflected wave from the nearby cylindrical walls grows to ~25MPa and travels along the y-axis in both directions. Figure 12(c) shows that this reflected wave meets at the location of y=~2cm, with the original detonation wave reflected at the dome wall. As a consequence of such an overlap, the pressure amplifies to above 50MPa, as seen in Figures 12(c) & (d). Figure 12(d) also shows that this high pressure wave dissipates quickly as it moves away from this location. Figure 13 shows pressure wave variation across the cross section near the boundary, y=-21cm. Figure 14 shows temporal variation of pressure at various locations along the vacuum tube wall. As seen in the case 1, the reflected wave varies around 10 to 15MPa. When the secondary wave comes in and is reflected at the wall near the tracer point 1, however, the magnitude becomes ~30MPa. This is because the wave overlapping and focusing occurs much closer to the wall as seen in Figures 12(c) & (d). At all other locations, the reflection of the secondary wave is much smaller than the primary reflection. It is unclear whether the near-wall pressure will increase if the detonation location is moved away further from the location assumed in the case 2 study. If not, the case 2 study is

conservative and definitive. Otherwise, it is recommended to repeat the similar study assuming detonation initiation at different locations. In the middle of the gas mixture, the secondary wave is also shown to be large in Figure 15. Temperature variations are shown in Figures 16 and 17. The gas mixture temperature near the wall is about ~3000K as it burns. Peak temperature at the tracer point 1 is about 4000K as the secondary compressive wave comes in.

3.3 Case 3 Results - Multiple Volumetric Detonations

To simulate the effect of volumetric detonation, 20 detonation points were distributed at every 2.5cm interval through the vacuum tube. It was assumed that detonation starts at all 20 locations simultaneously. Figures 18 through 22 show pressure and temperature variations at various locations and time. Pressure waves are overlapped and focused at various locations as shown in Figure 18(a). These waves are seen to diminish in Figures 18(b) & (c), and grow again as seen in Figure 18(d). As seen in other case studies, the pressure in the gas mixture near the wall vary around 10MPa except for the tracer point 1 where the secondary pressure peaks above 30MPa. Temperatures at various locations also shown in Figures 21 and 22, vary around 3000K except for the point 1 where the temperature rises as high as 5000K as the compression wave comes in contact with the wall.

3.4 One-Dimensional Simulation of Case 1

Two-dimensional simulation of the case 1 was repeated with 1-D simplification as shown in Figure 23. As seen in the figure, at one end, the aluminum wall was modeled with the same thickness assumed in 2-D simulation. Also same initial conditions of 92K and 0.1MPa of the air/hydrogen stoichiometric mixture was assumed for the calculation. Outside and inside this vacuum tube wall are filled with air/gas mixture. Detonation region extends to ~ 2m which is about same length of the entire vacuum tube. A point detonation was assumed to start at 5.48cm away from the wall, the same location as we assumed in the case 1 study. Figure 24 illustrates temporal pressure variation at various tracer points shown in Figure 23. Since this pressure variation is in the middle of the gas mixture, these results should only be compared with the results reported in Figure 9 of the 2-D calculation of the case 1. It will be noted that the shock pressure rise in CTH is somewhat larger than that one gets from lumped parameter models as in CET89. This is due to the need in CTH to slightly increase the detonation velocity for ensuring that total combustion energy input into the system matches thermodynamic values (i.e., energy available from

hydrogen combustion). Another reason relates to the different calculational methods used in CTH versus CET89. Shock (CJ) pressures from CTH are obtained dynamically with continuous wave energy dissipation to surroundings along with continuous variations in physical properties of the environment (effects which are not present in point kinetics/lumped approaches). Regardless of the minor variations in the CTH shock pressures from lumped model simulations, total energy is properly conserved. From Figure 24(a), it is seen that the reflected pressure is ~13 MPa (tracer point 1), which is similar the magnitude estimated from 2-D study of the case 1 (pressure at the tracer point 1 shown in Figure 8(a)). About 7MPa of initial detonation wave is followed by ~4MPa of dissipating reflected secondary wave (tracer points 4 and beyond). However, this 1-D calculation revealed the secondary wave is much smaller to compare with that shown in Figure 9 of 2-D calculation. Also the third wave is not possible to be created in the 1-D simulation whereas it is clearly seen in the 2-D simulation as shown in Figure 9. In these 1-D calculations, pressure wave focusing and overlapping are not present since multi-dimensional geometrical effects are not represented. The secondary reflected wave in this 1-D calculation is shown to be submerged into the equilibrium pressure as the wave travels far and dissipates as shown in Figure 24(c).

4. Summary and Conclusion

Three cases of different detonation locations were studied for same initial conditions of 92K and 0.1MPa for a stoichiometric air/hydrogen mixture. Case 1 assumes a detonation initiated at r=0 and y=0 point. A point detonation initiated at the location of r=0 and y=-10cm is the case 2. Case 3 simulates volumetric detonation with multiple simultaneous detonation points. Also 1-D calculation was made for the similar case as the case 1. When the detonation initiates at the center of the hemispherical cap of the vacuum tube as in the case 1, the maximum pressure imposed to the wall was estimated at ~12.5MPa near the nose tip portion of the vacuum tube cap. The other cases show that at the same location, the maximum pressure loading can be as high as ~30MPa. The maximum pressure loading at the wall always occurs at the tracer point 1. As the initial detonation point moves away from the point assumed for the case 1, the maximum pressure in the gas mixture occurs closer to the wall near the nose tip of the vacuum tube cap. The primary detonation wave proceeds with a magnitude of ~5~6MPa and passes away from the system boundary, y=-21cm. This wave is assumed to keep proceeding until it impacts the neutron window. Upon impacting the window, it is reasonable to assume the reflected wave to be about 12MPa. The secondary wave from the case 2 is seen to be ~25MPa when it moves out of the system boundary whereas the case 1 shows about 15MPa. This wave from the case 2

may dissipate to a similar magnitude as that for case 1 as it keeps traveling down the tube. This secondary pressure of 15MPa can further dissipate as it moves downwards. Without extensive geometry modeling of the entire length of the vacuum tube, it appears conservative to assume that the secondary wave reaches a level of ~15MPa as it impacts the neutron window. However, one should note that this is a focused pressure wave along the center line. Temperatures of the gas mixture is another concern. The gas temperature near the structure wall remains at ~3000K for a significant period of time. Inner surface of the tube wall will be heated to a high temperature while outer wall remains cold. Thermal stress due to such a large temperature difference across the wall needs to be assessed.

5. References

[1] S. Gordon and B.J. McBride, "Computer program for calculation of complex chemical equilibrium compositions, rocket perfromance, incident and reflected shocks, and Chapman-Jouguet detonations," Spec. Publ. NASA SP-273, March 1976 (Lewis Research Center, NASA)

[2] J.M. McGlaun and S.L. Thompson, "CTH: a three-dimensional shock-wave physivs code," Int. J. of Impact Eng., 10 (1990) 251-360

[3] R.K. Byers, "CSQ calculations of H2 detonations in the Zion and Sequoyah nuclear plants," Rep. NUREG/CR-2385, July 1982

[4] R.P. Taleyarkhan, and et. al., "Modeling and analysis of hydrogen detonation events in the advanced neutron source reactor containment," J. of Nuclear Eng. Design 166 (1996) 471-480

[5] D.C. Willams, and et. al., "Containment loads scoping calculations for severe nuclear reactor accidents," SAND92-2774, NPRW-SA90-5, Sandia National Laboratories, February 1993

[6] L.W. Boyack, and et. al., "Loads from the detonation of hydrogen-air-steam mixtures," SAND92-0541, Sandia National Laboratories, July 1992

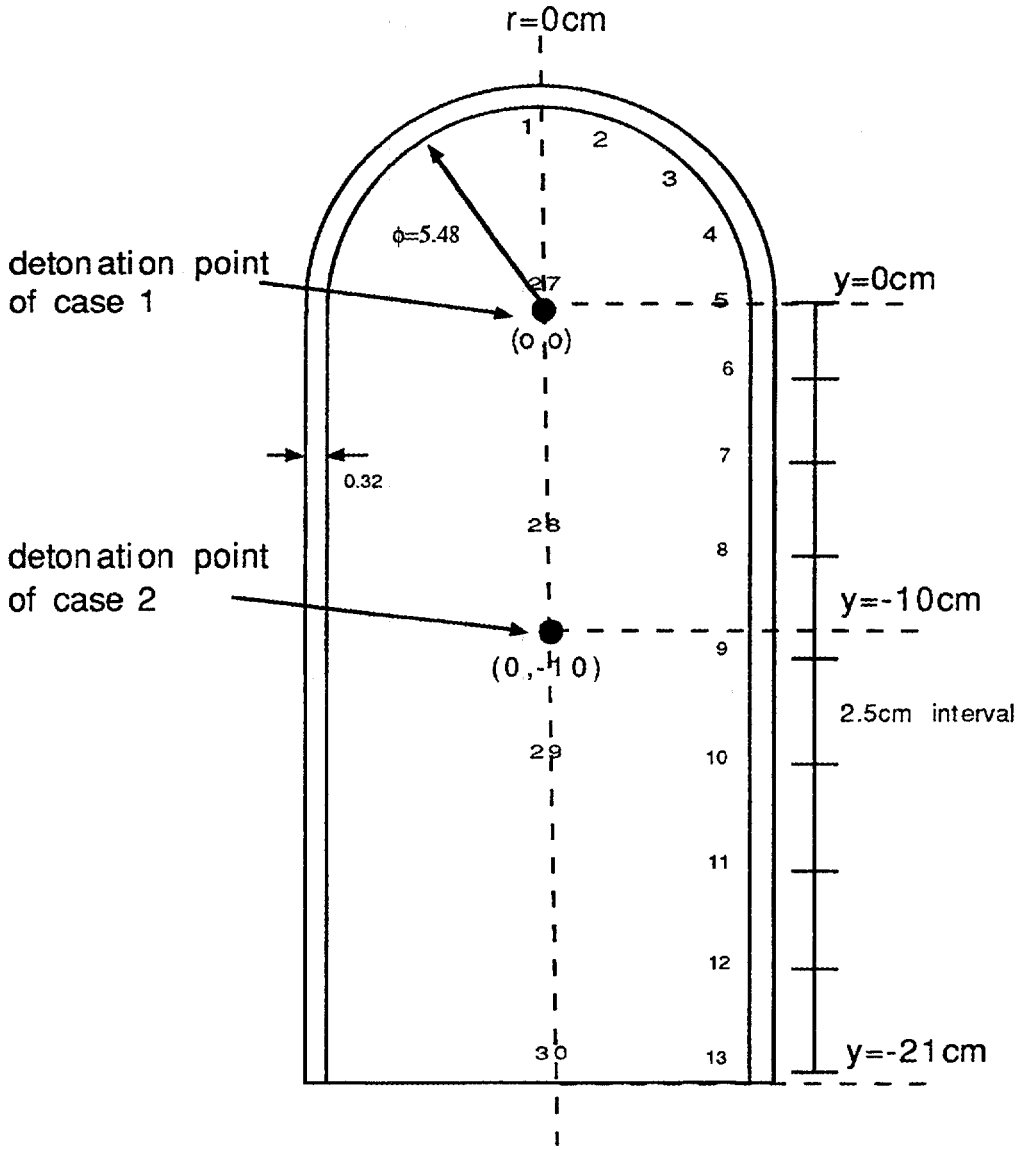

Figure 4. Vacuum Tube Modeled for CTH calculations with Tracer Points

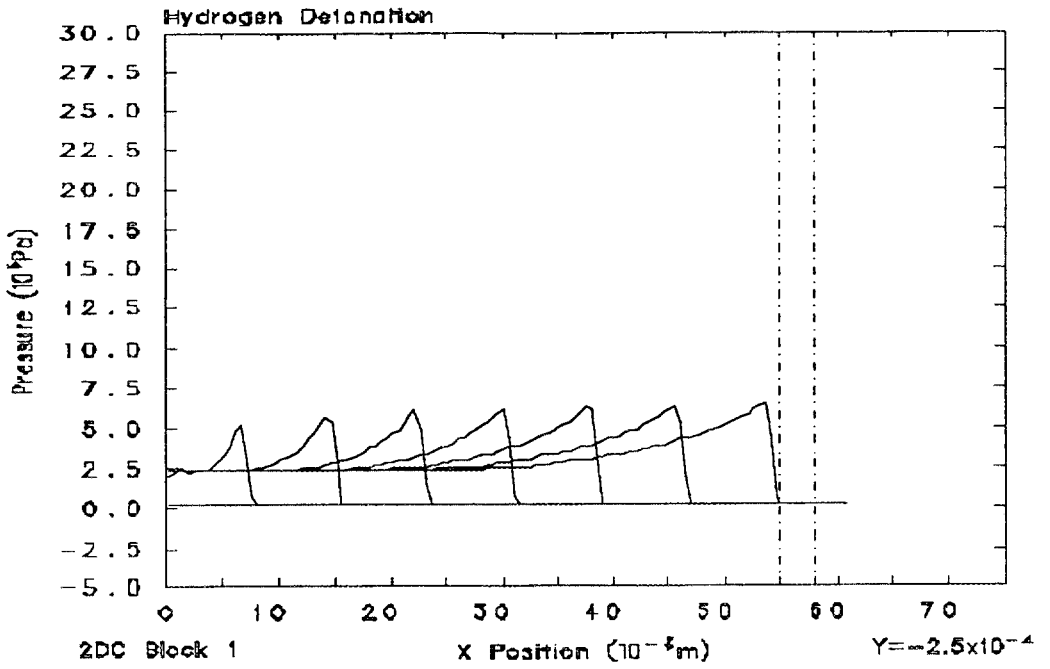

Figure 5(a). Pressure profile along y=0 line from 0 to 21μsec with 3μsec time interval for case 1

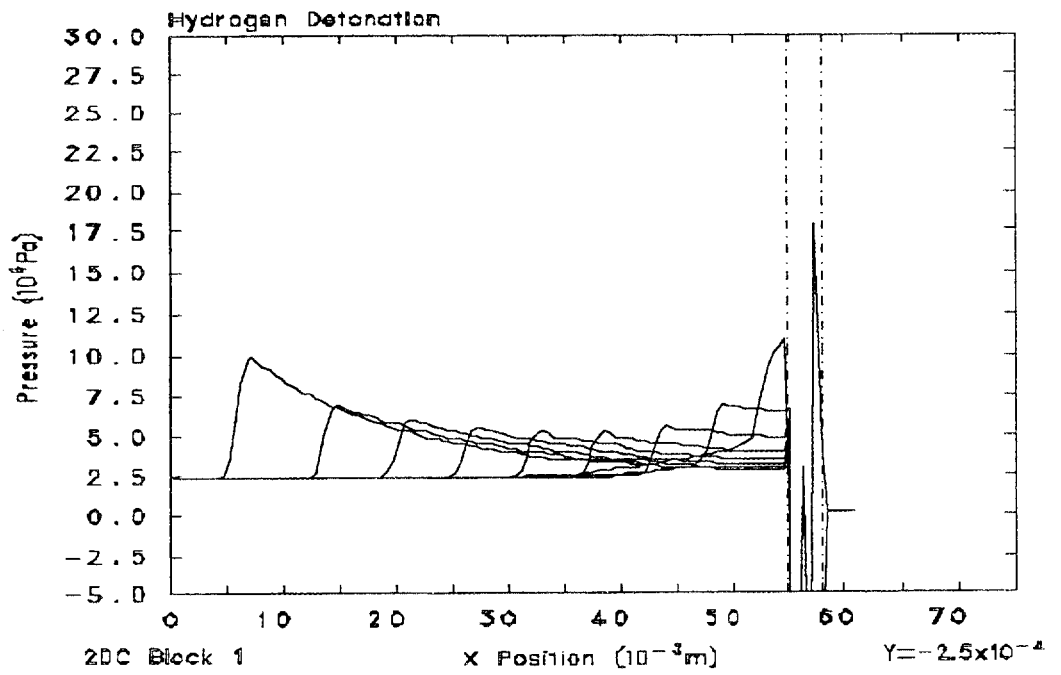

Figure 5(b). Pressure profile along y=0 line from 23 to 47μsec with 3μsec time interval for case 1

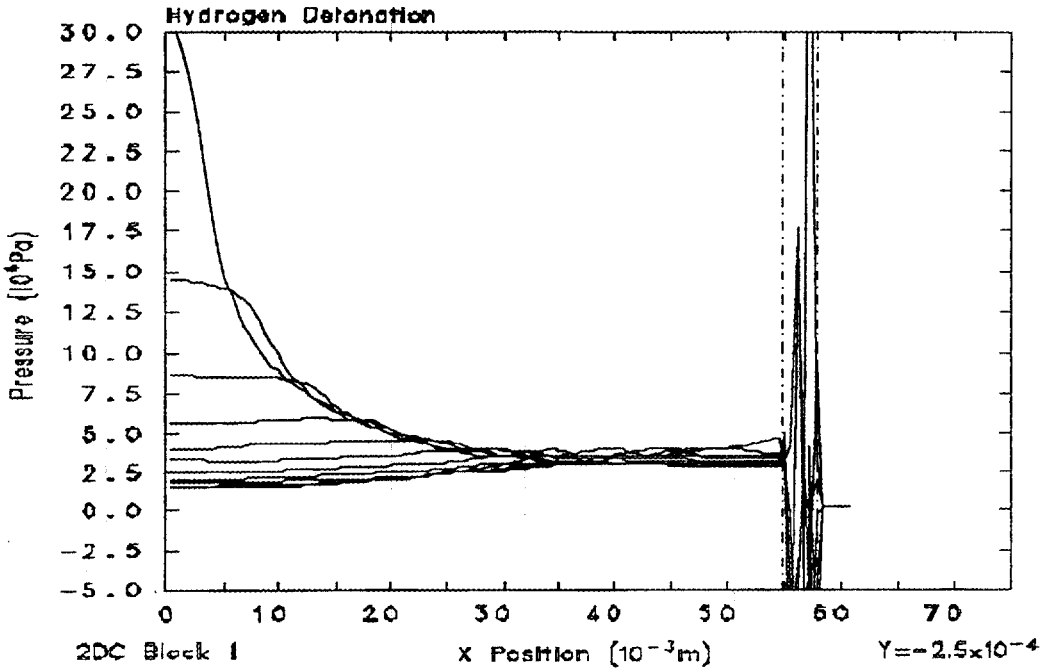

Figure 5(c). Pressure profile along y=0 line from 49 to 79μsec with 3μsec time interval for case 1

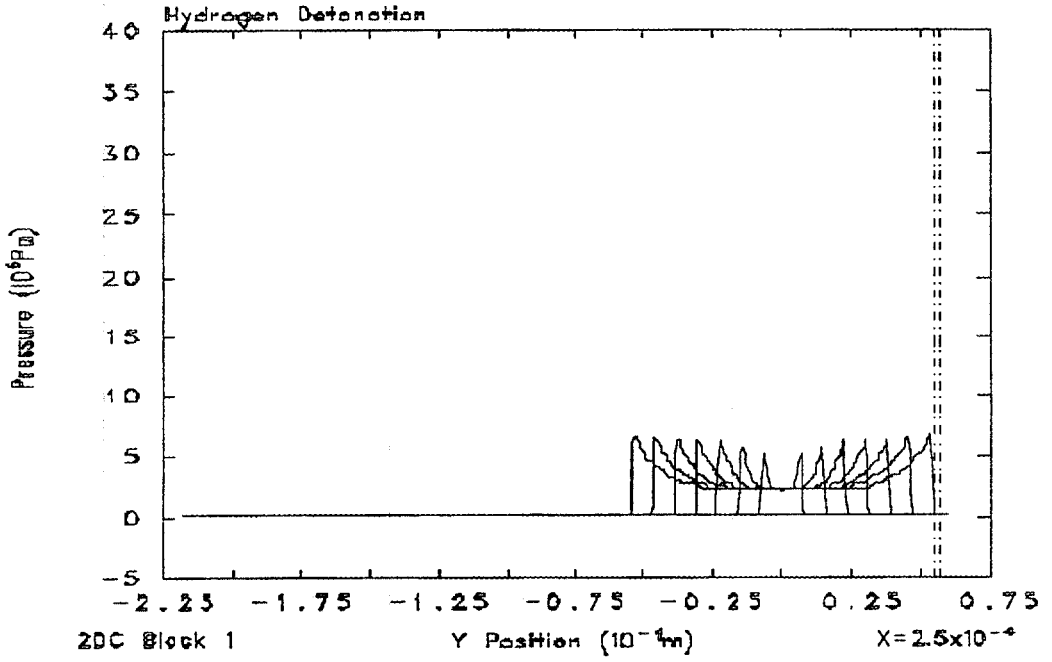

Figure 6(a). Pressure profile along r=0 line from 0 to 21μsec with 3μsec time interval for case 1

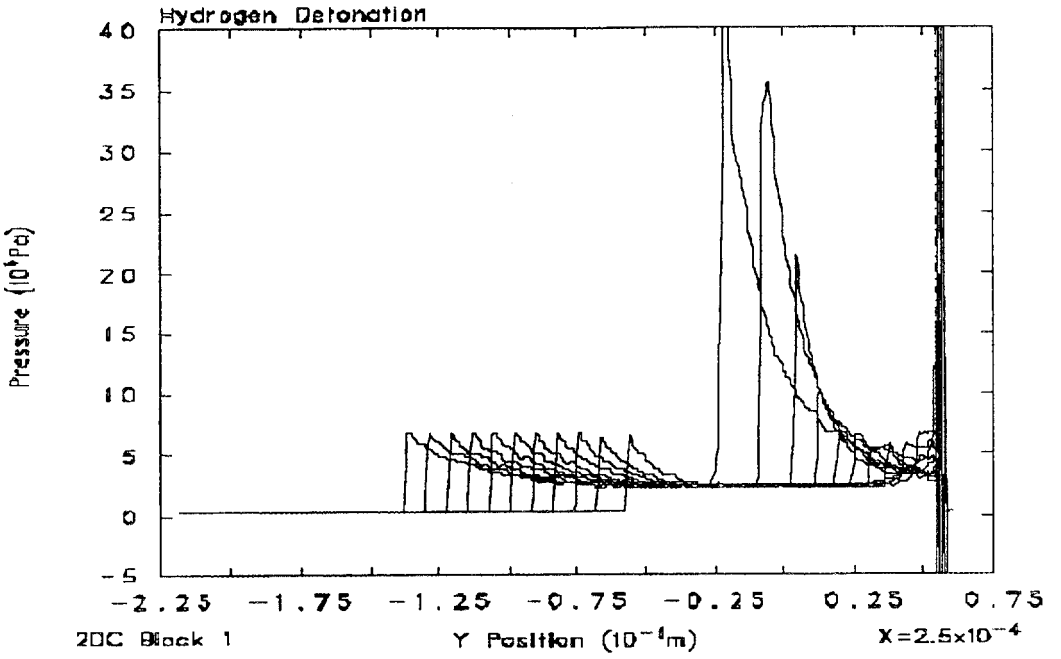

Figure 6(b). Pressure profile along r=0 line from 22 to 53μsec with 3μsec time interval for case 1

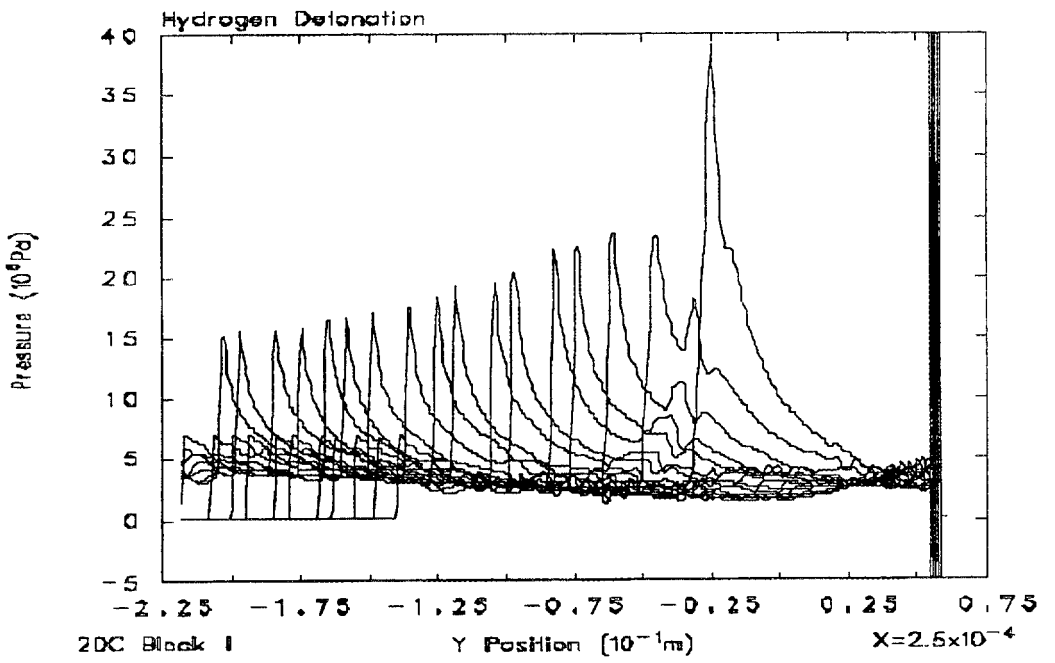

Figure 6(c). Pressure profile along r=0 line from 54 to 101μsec with 3μsec time interval for case 1

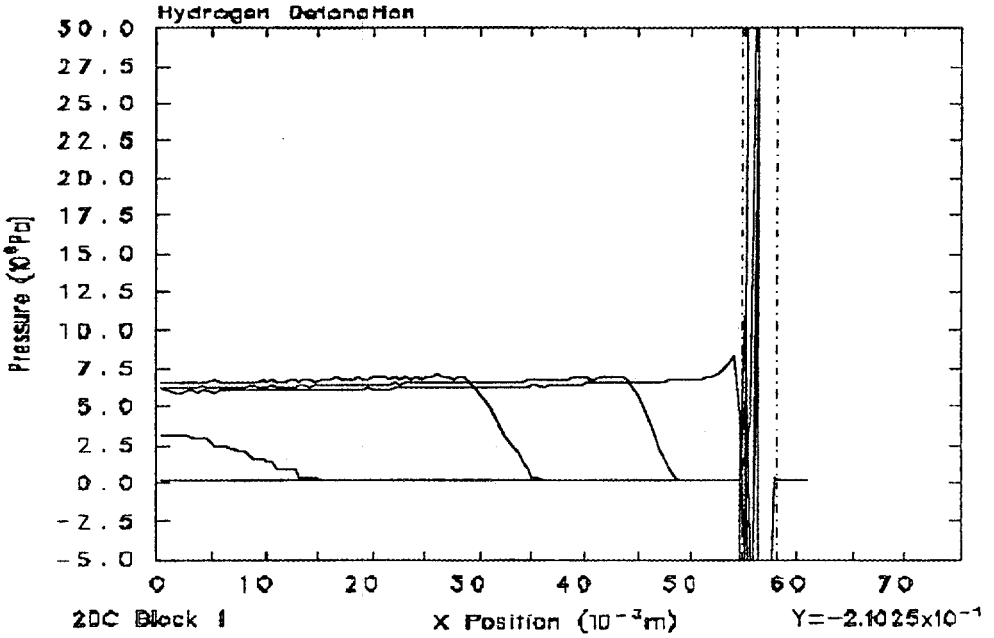

Figure 7(a). Pressure profile along y=-21 line from 80 to 84μsec with 1μsec time interval for case 1

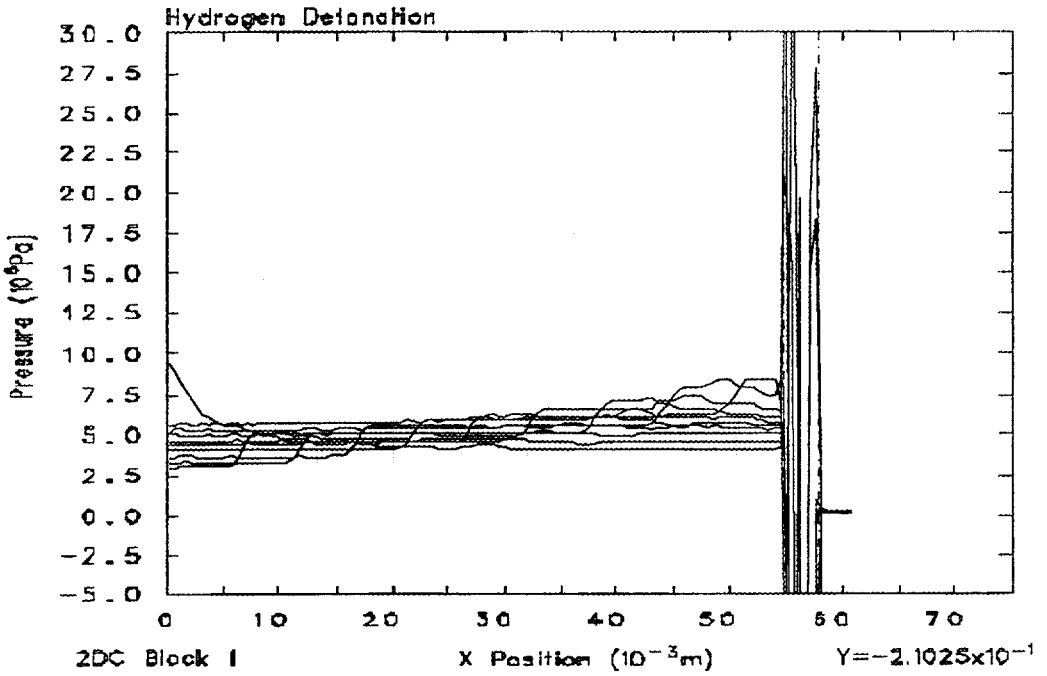

Figure 7(b). Pressure profile along y=-21 line from 85 to 103μsec with 2μsec time interval for case 1

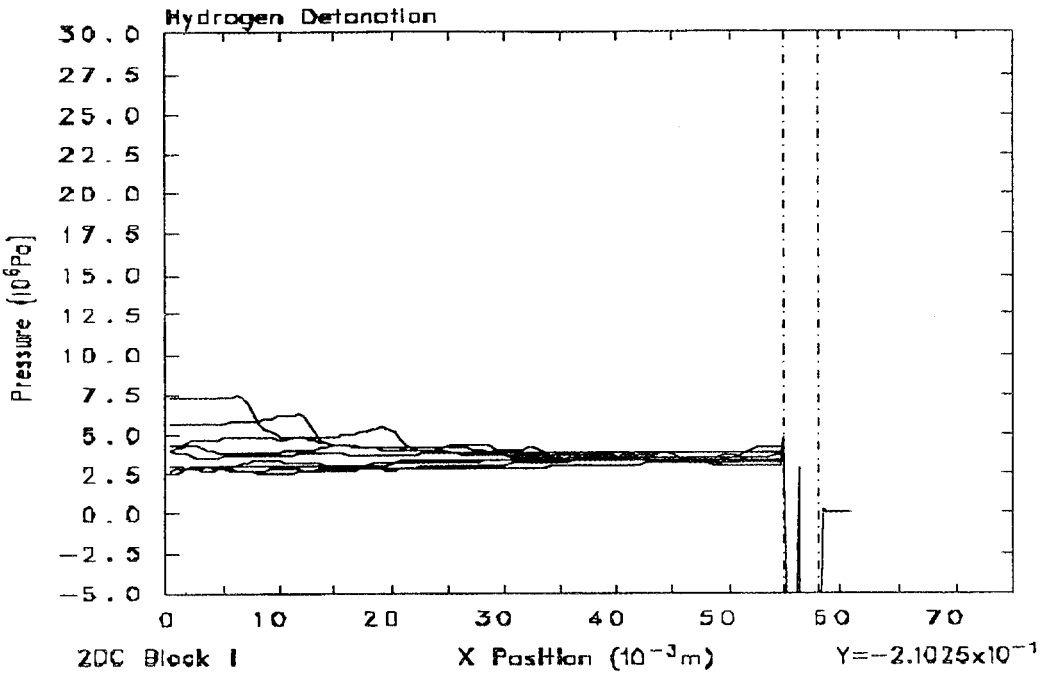

Figure 7(c). Pressure profile along y=-21 line from 104 to 129μsec with 3μsec time interval
for case 1

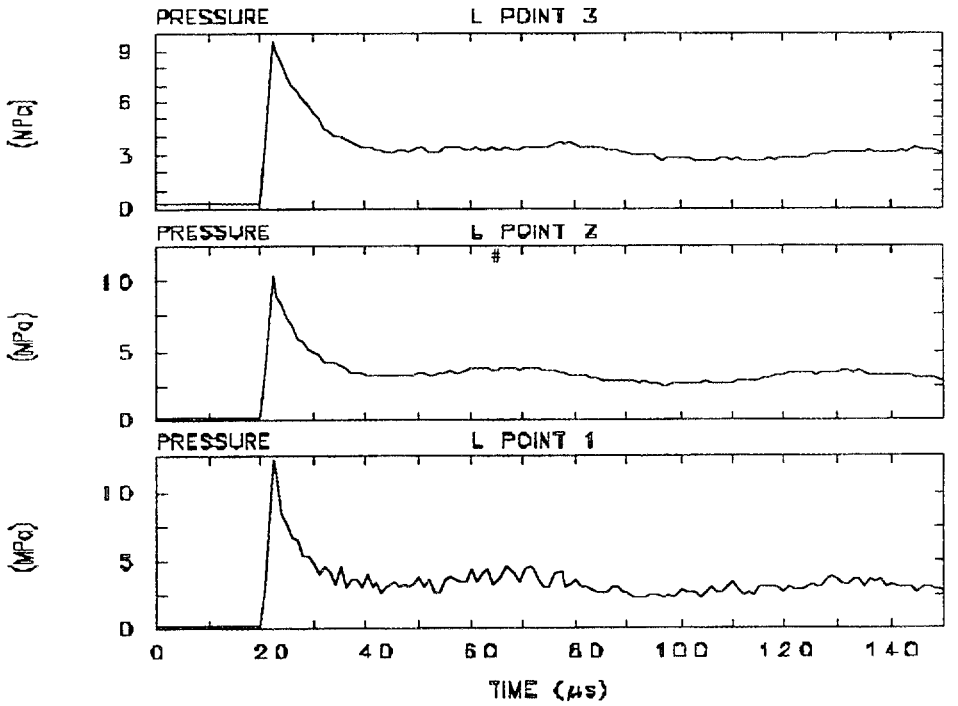

Figure 8(a). Pressure history in hydrogen/air mixture near the vacuum tube wall of case 1

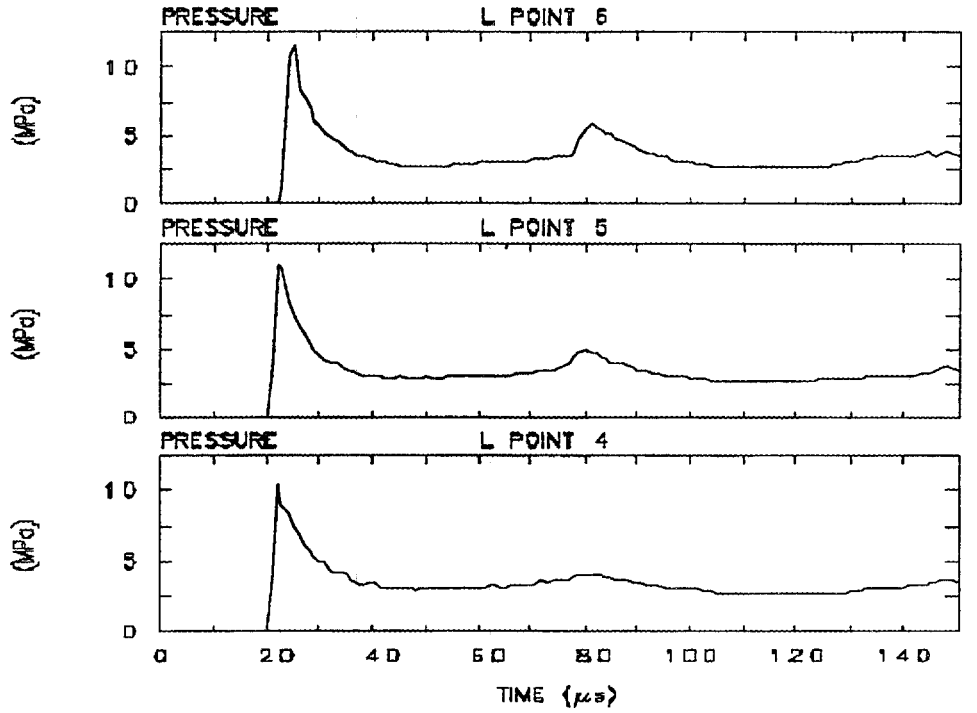

Figure 8(b). Pressure history in hydrogen/air mixture near the vacuum tube wall of case 1

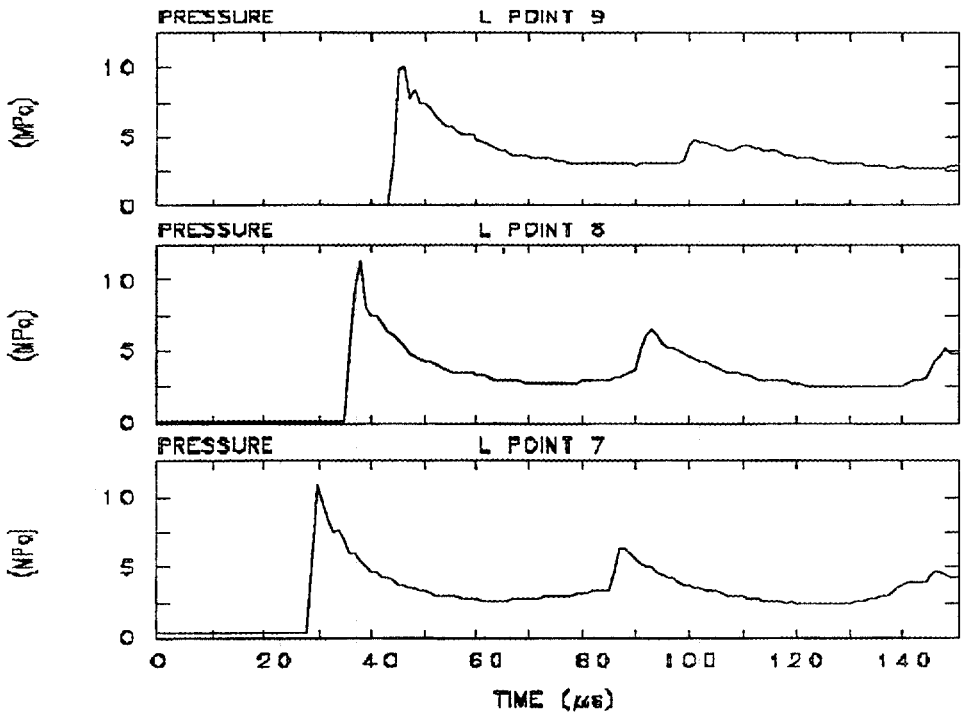

Figure 8(c). Pressure history in hydrogen/air mixture near the vacuum tube wall of case 1

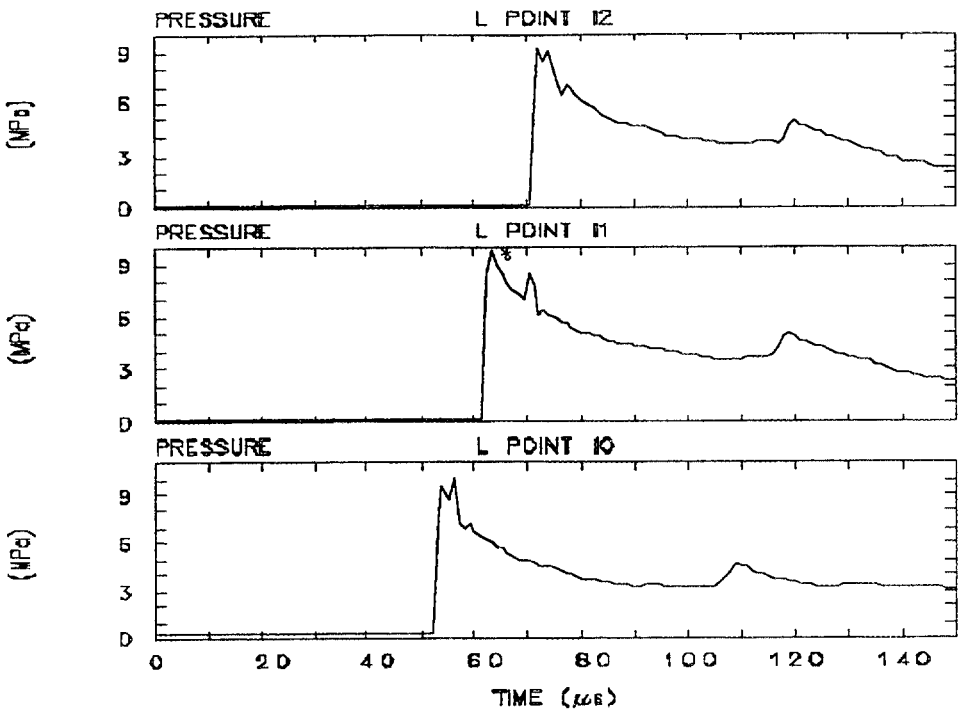

Figure 8(d). Pressure history in hydrogen/air mixture near the vacuum tube wall of case 1

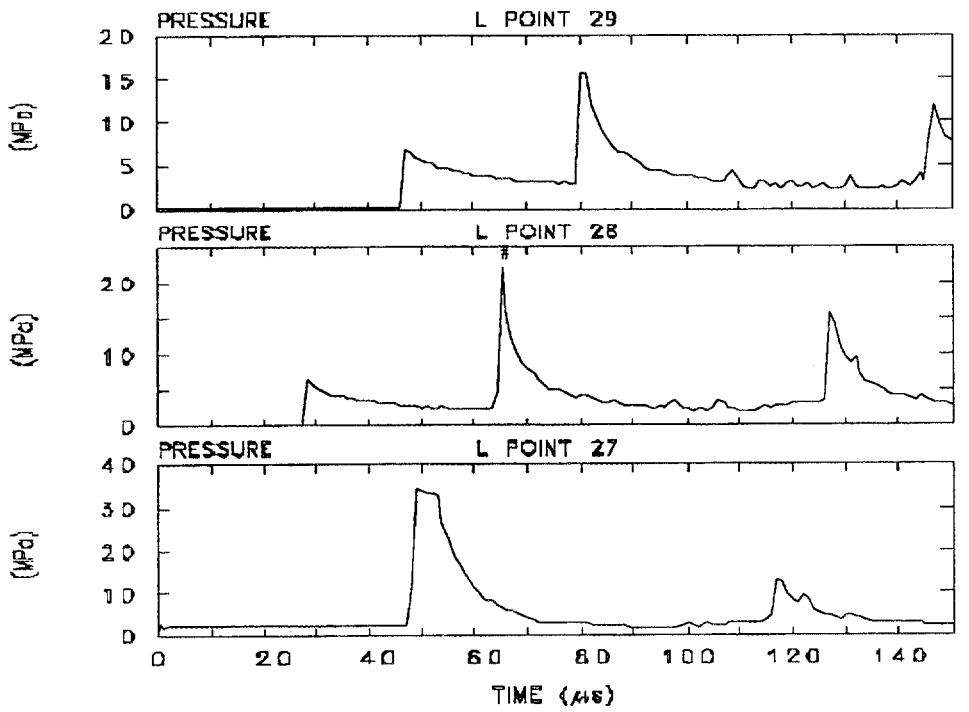

Figure 9. Pressure history in hydrogen/air mixture along r=0 of case 1

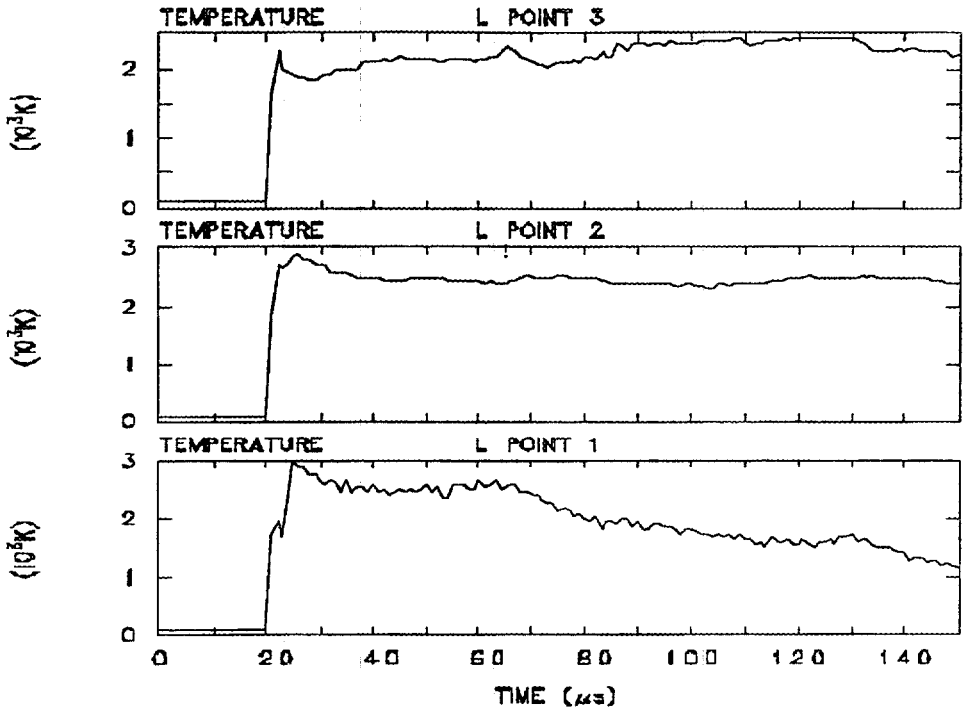

Figure 10(a). Temperature in hydrogen/air mixture near the vacuum tube wall of case 1

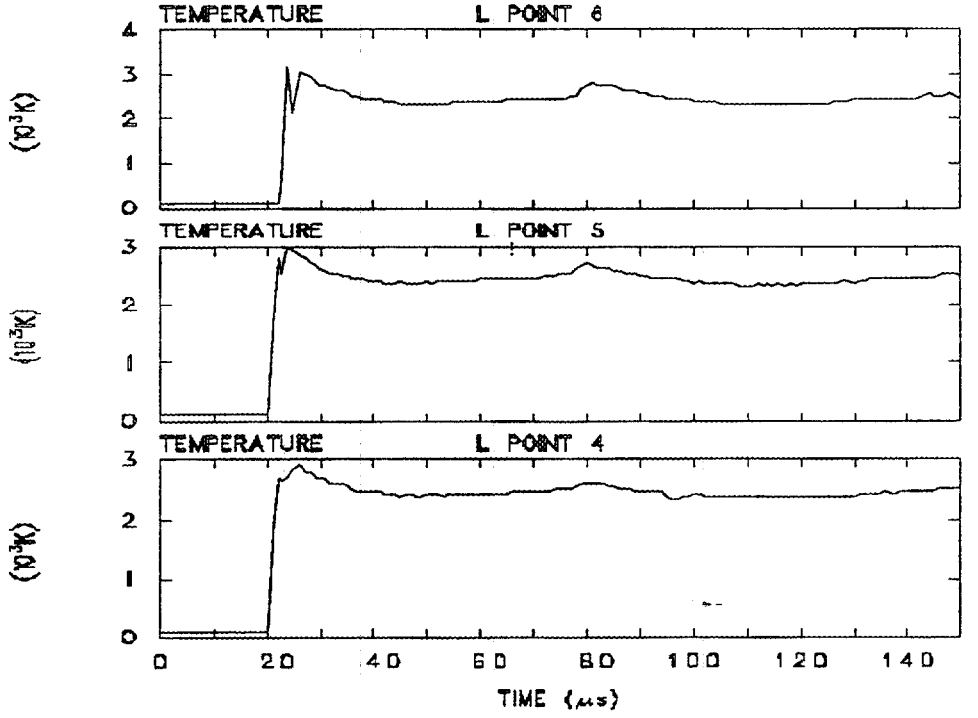

Figure 10(b). Temperature in hydrogen/air mixture near the vacuum tube wall of case 1

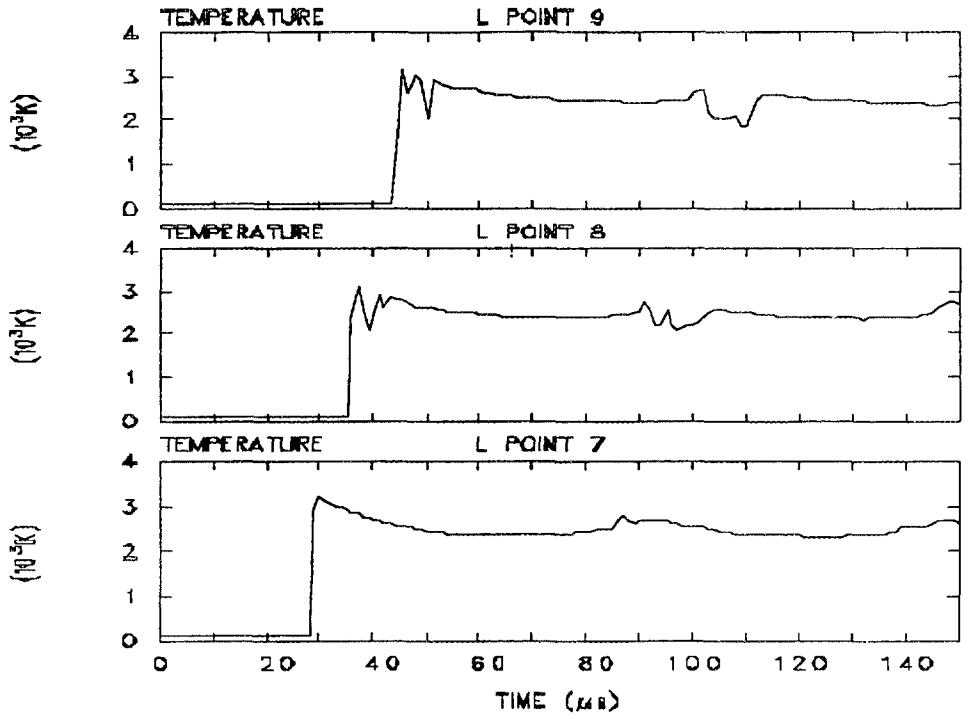

Figure 10(c). Temperature in hydrogen/air mixture near the vacuum tube wall of case 1

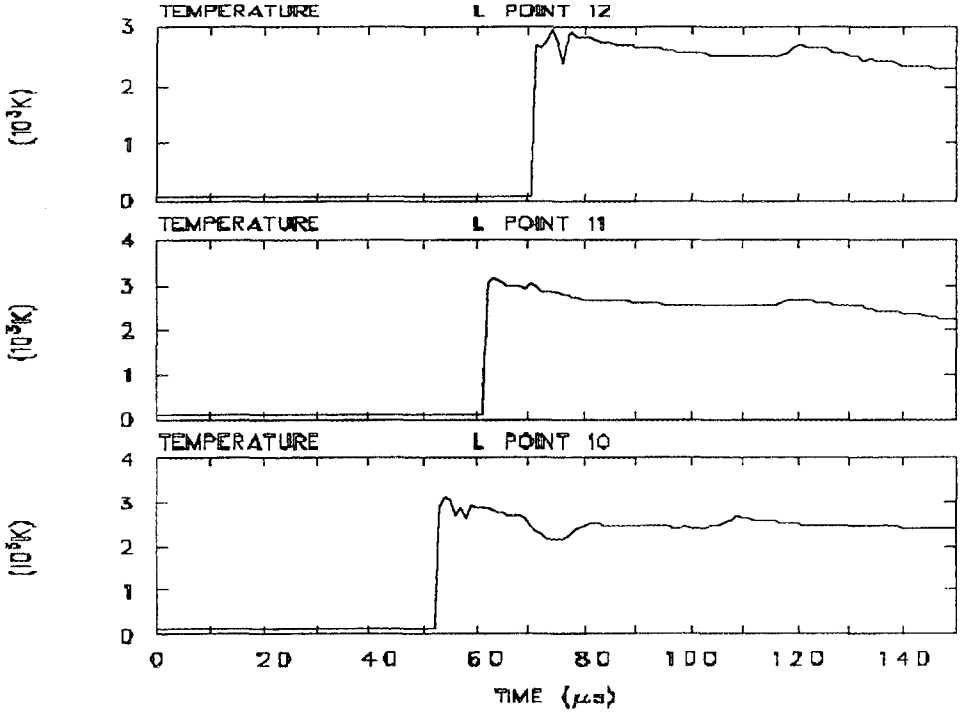

Figure 10(d). Temperature in hydrogen/air mixture near the vacuum tube wall of case 1

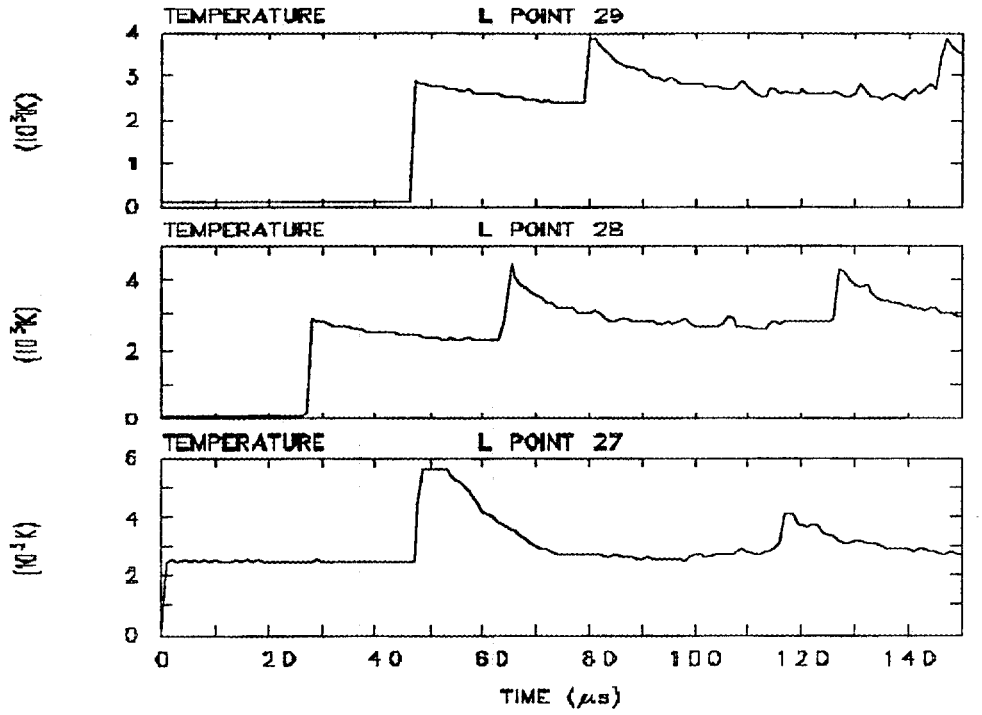

Figure 11. Temperature history in hydrogen/air mixture along r=0 of case 1

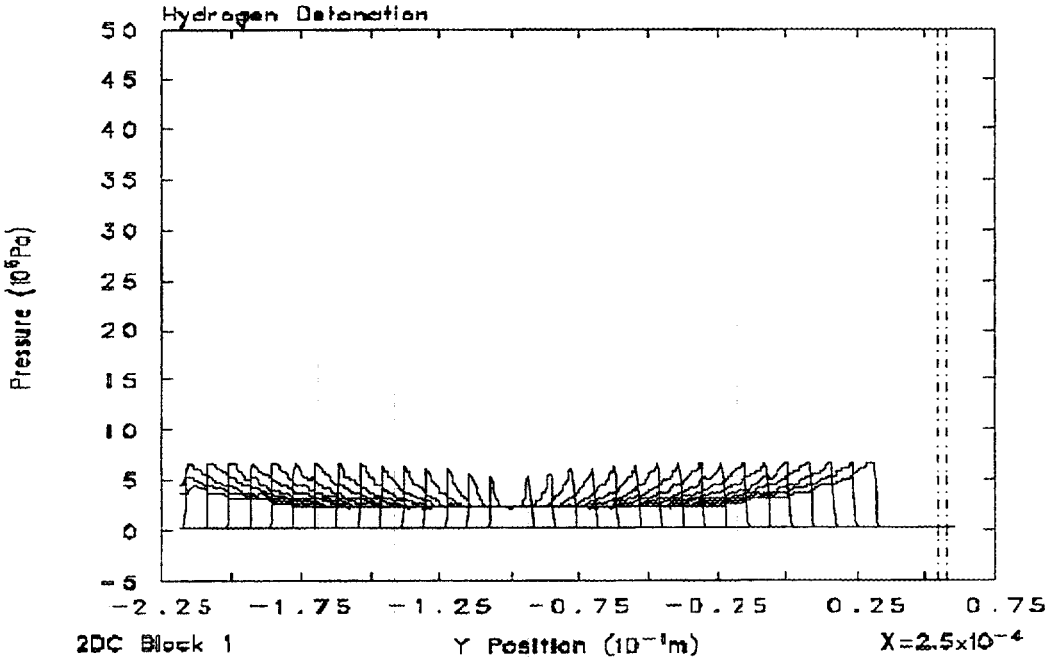

Figure 12(a). Pressure profile along r=0 line from 0 to 51μsec with 3μsec time interval for case 2

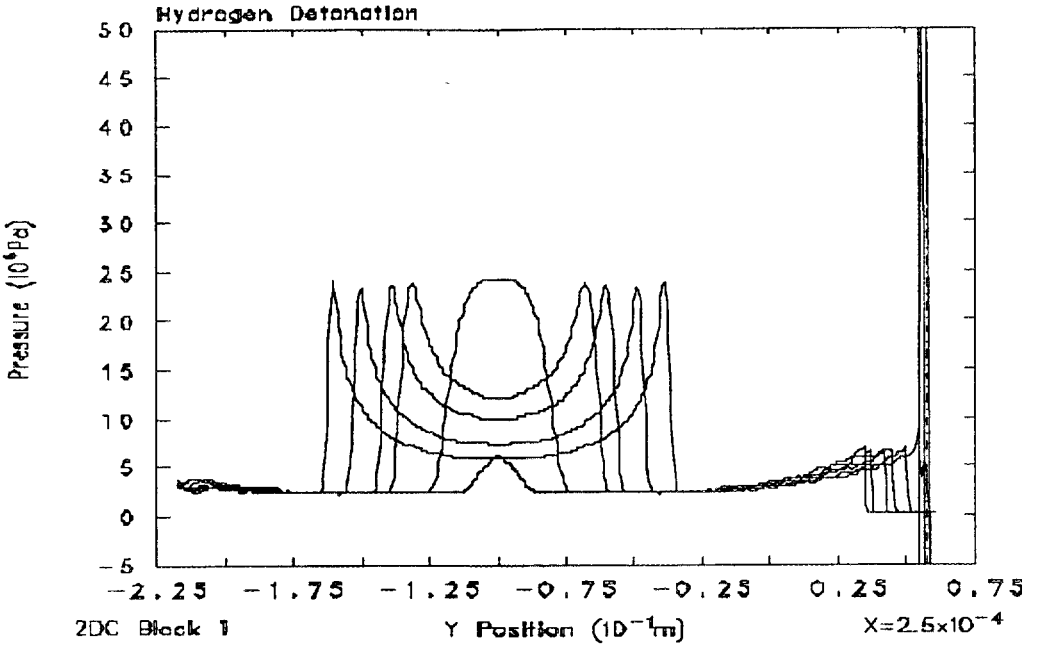

Figure 12(b). Pressure profile along r=0 line from 52 to 61μsec with 2μsec time interval for case 2

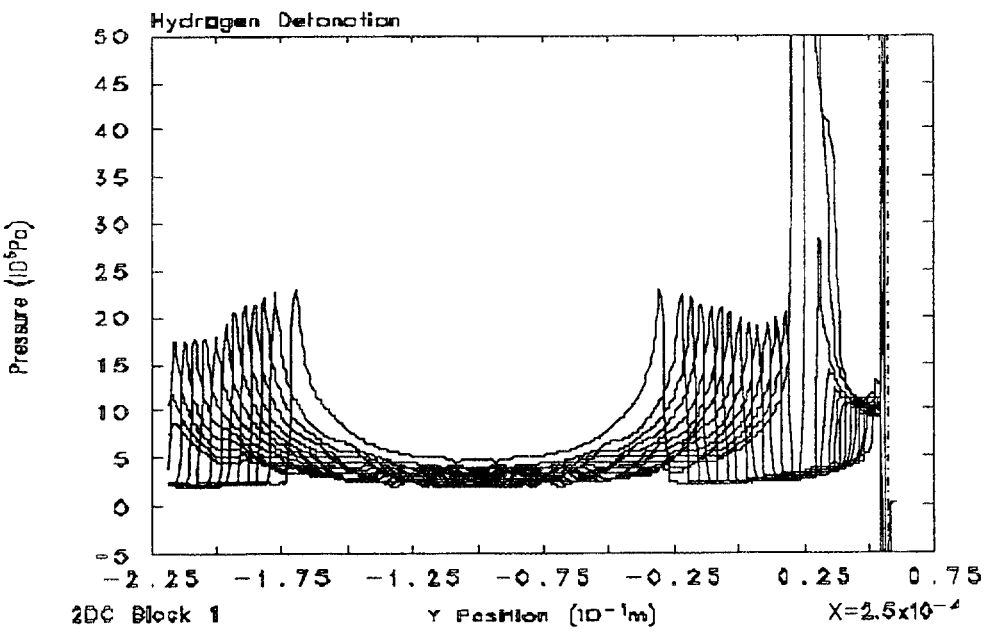

Figure 12(c). Pressure profile along r=0 line from 62 to 76μsec with 1μsec time interval for case 2

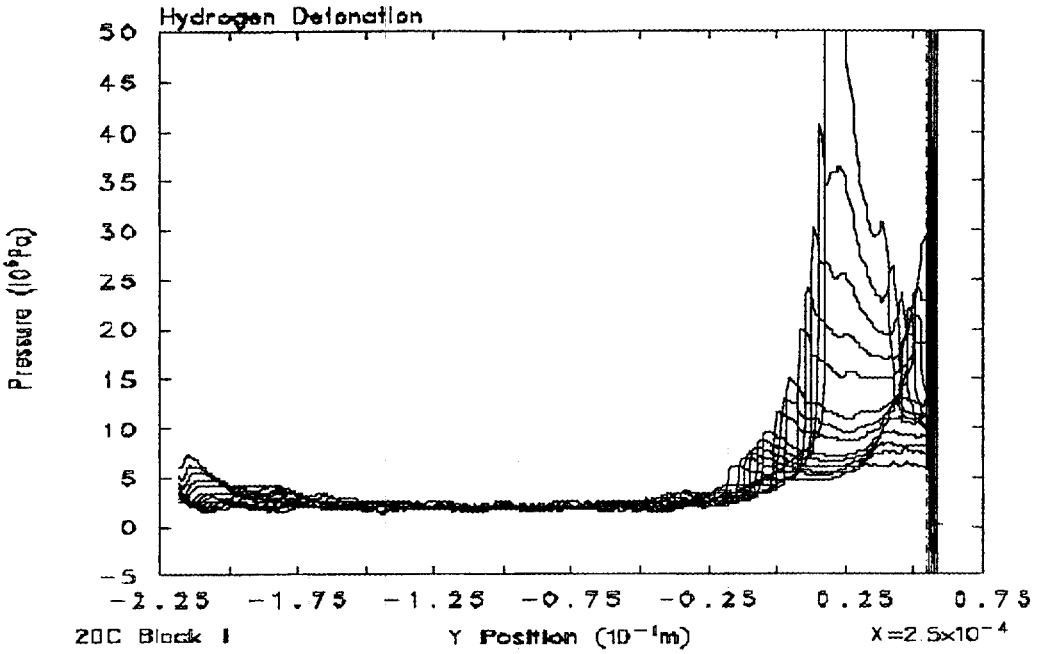

Figure 12(d). Pressure profile along r=0 line from 77 to 93μsec with 1μsec time interval for case 2

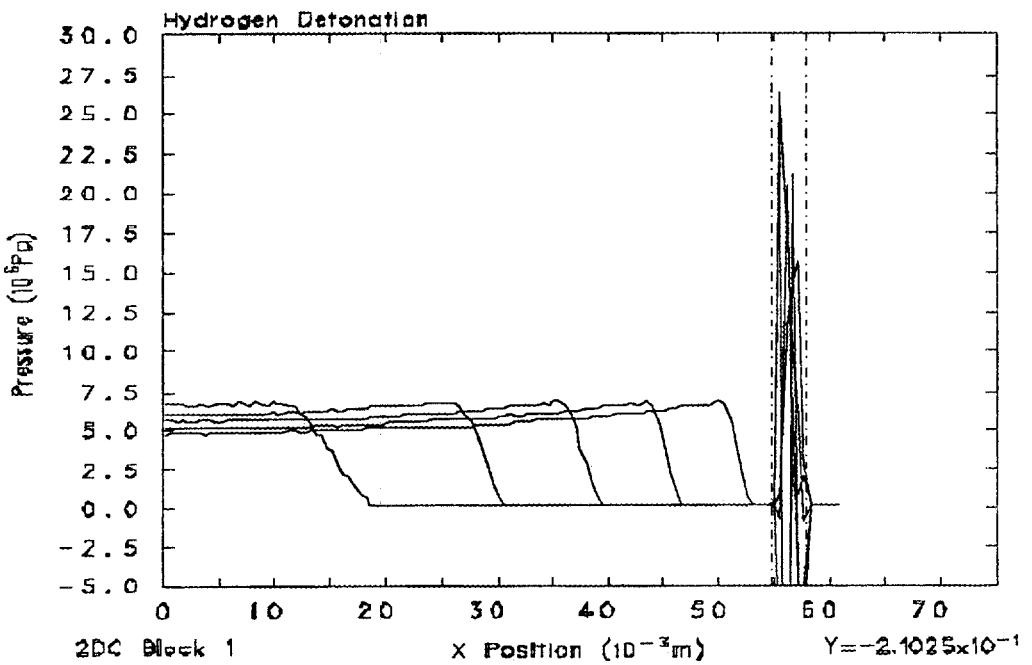

Figure 13(a). Pressure profile along y=-21 line from 42 to 48μsec with 1μsec time interval for case 2

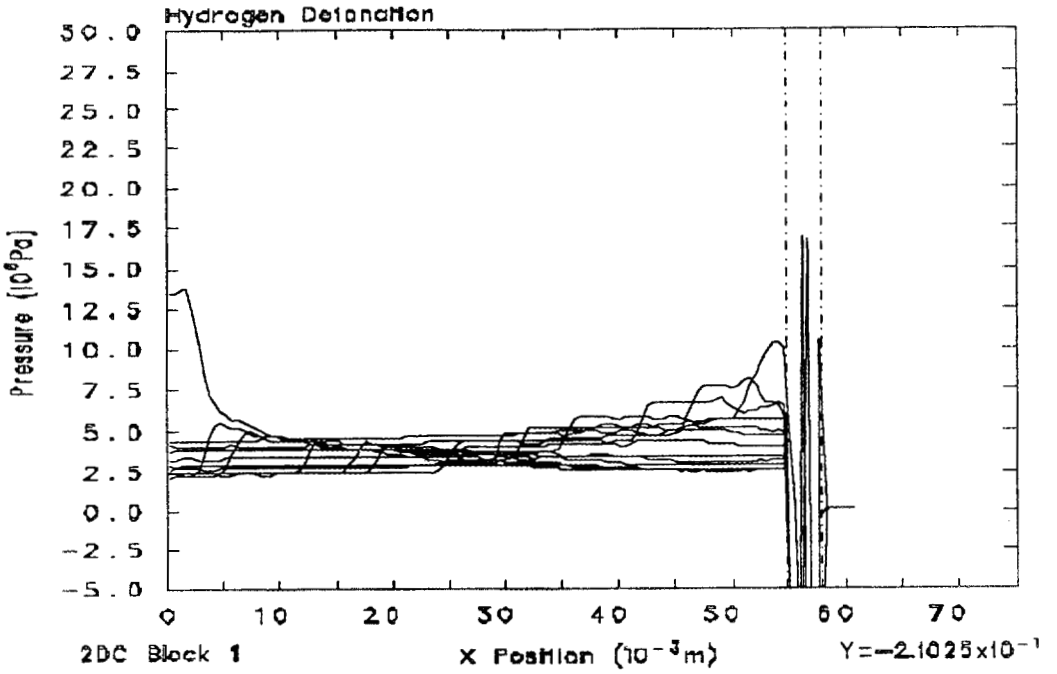

Figure 13(b). Pressure profile along y=-21 line from 49 to 73μsec with 3μsec time interval for case 2

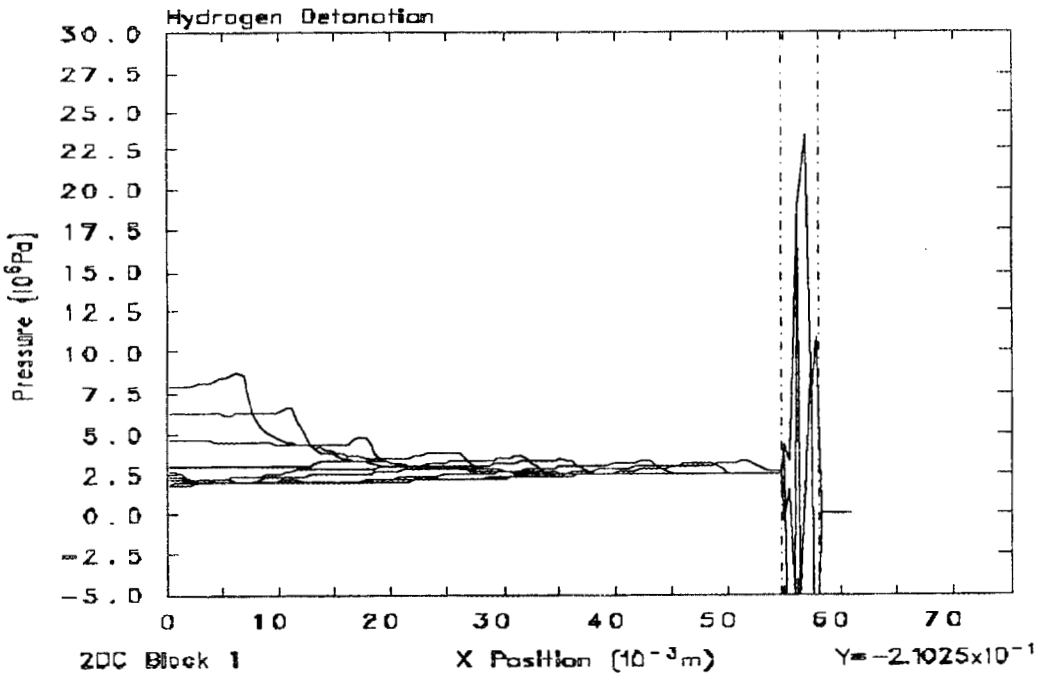

Figure 13(c). Pressure profile along y=-21 line from 74 to 100μsec with 3μsec time interval for case 2

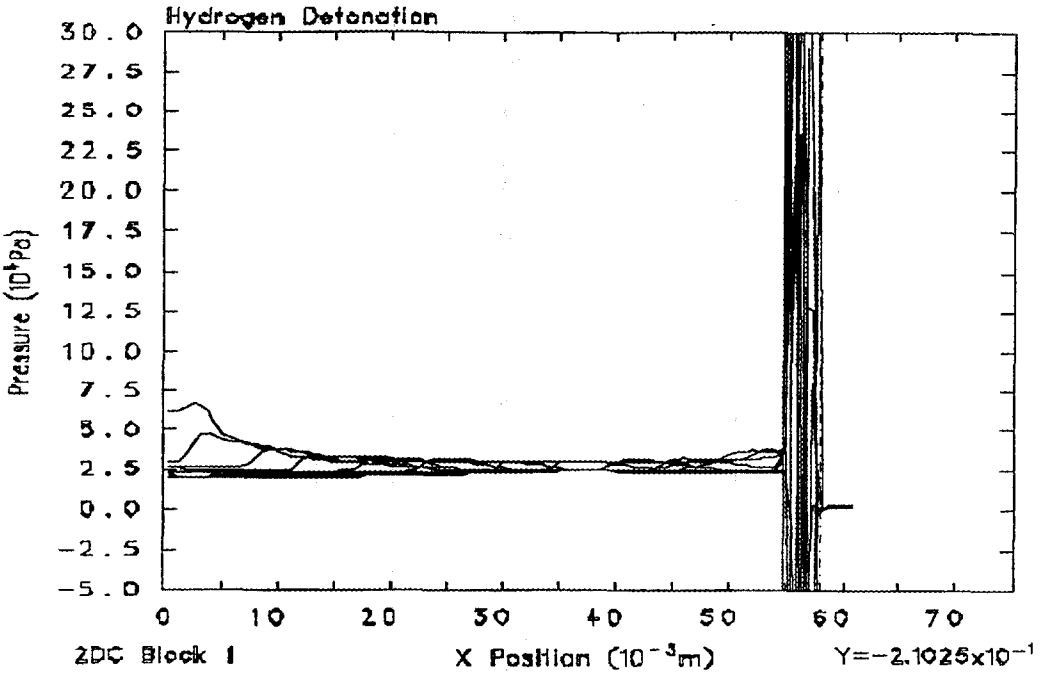

Figure 13(d). Pressure profile along y=-21 line from 101 to 133μsec with 3μsec time interval for case 2

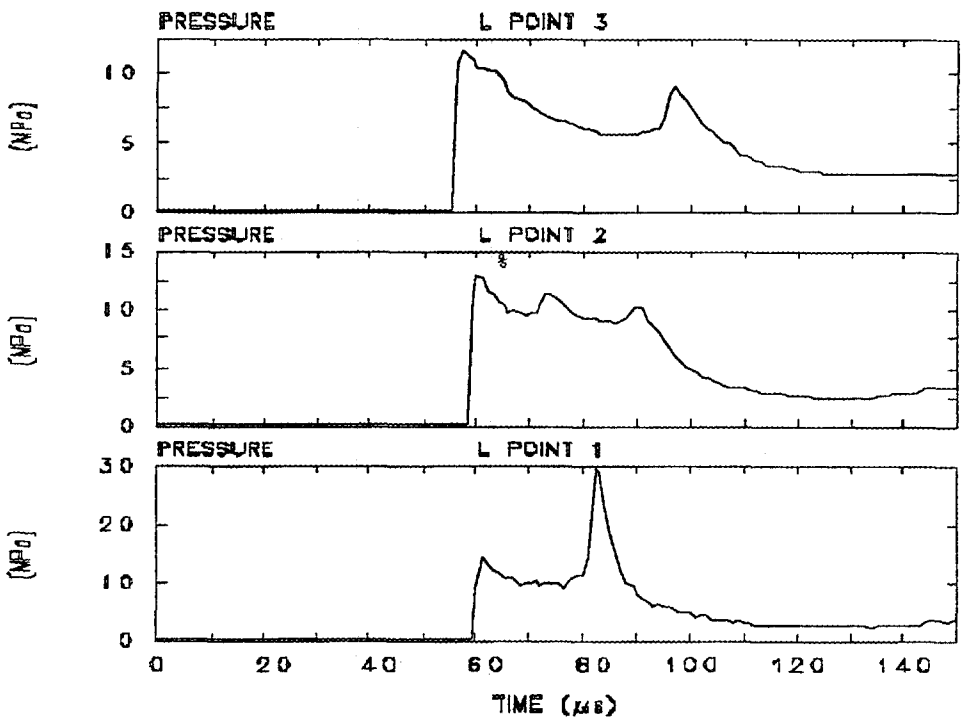

Figure 14(a). Pressure history in hydrogen/air mixture near the vacuum tube wall of case 2

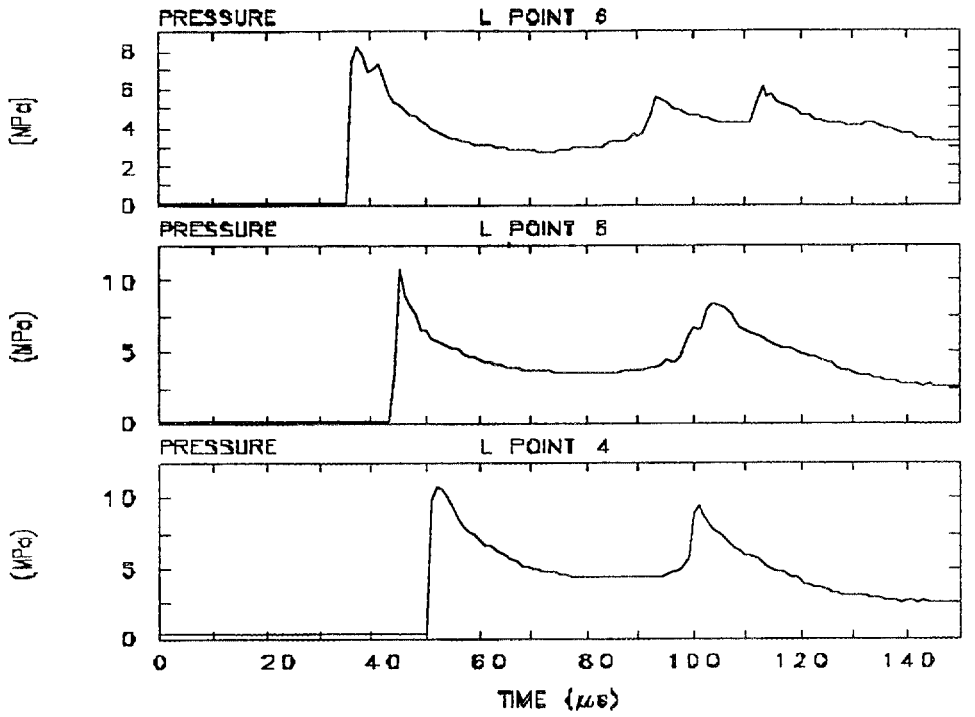

Figure 14(b). Pressure history in hydrogen/air mixture near the vacuum tube wall of case 2

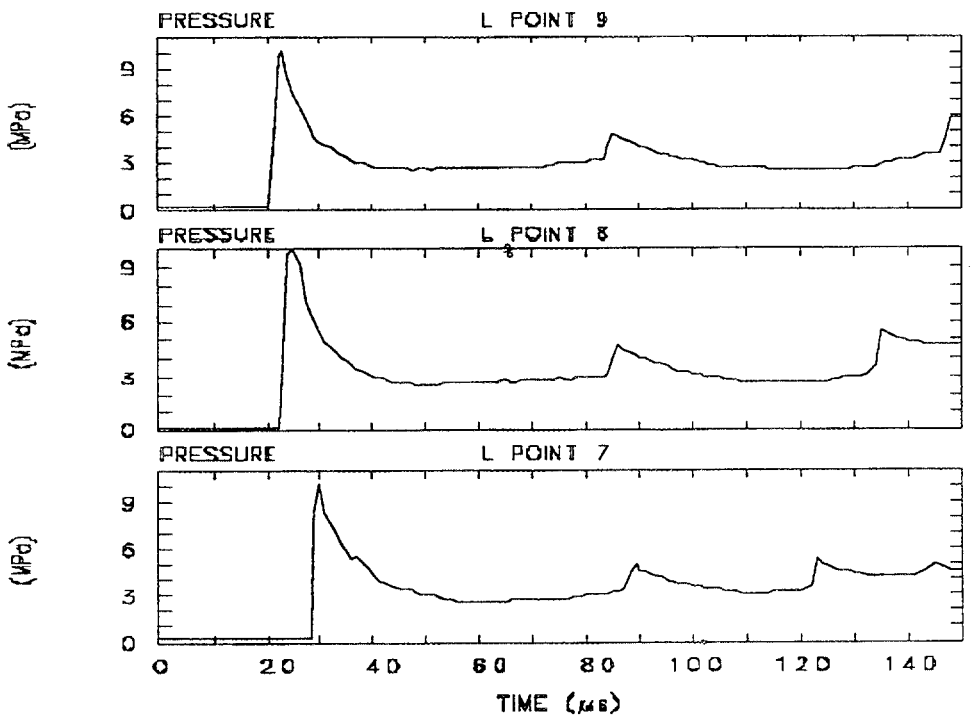

Figure 14(c). Pressure history in hydrogen/air mixture near the vacuum tube wall of case 2

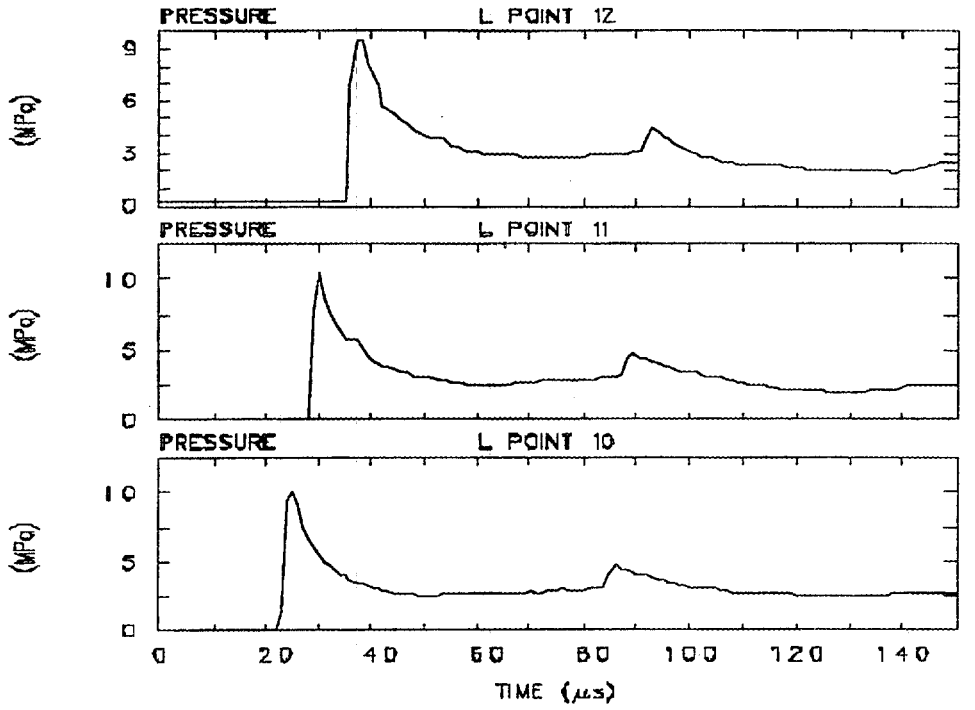

Figure 14(d). Pressure history in hydrogen/air mixture near the vacuum tube wall of case 2

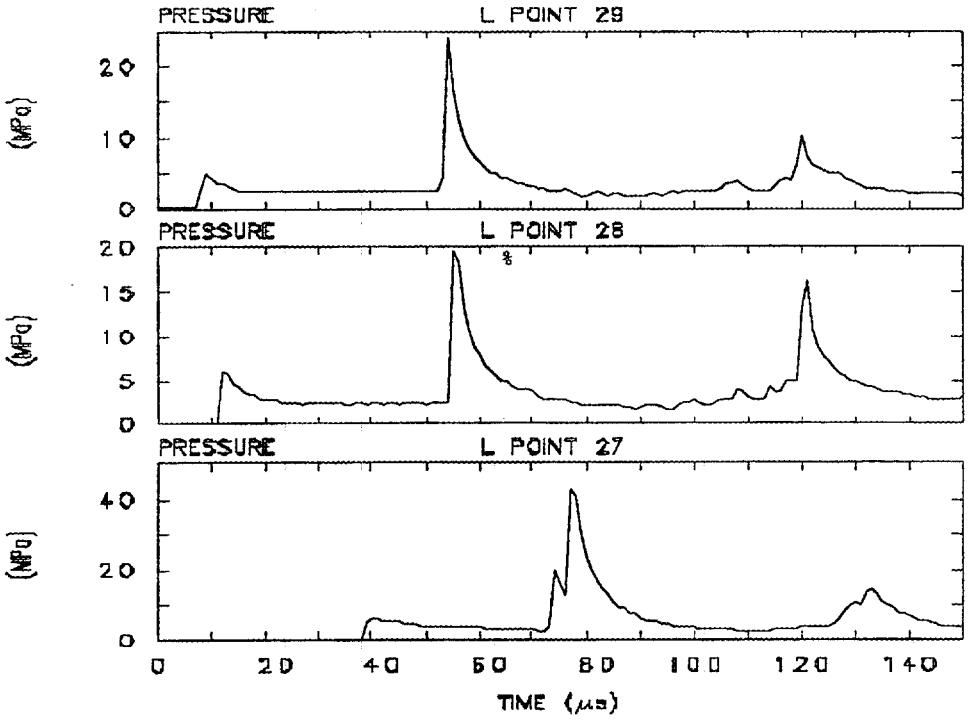

Figure 15. Pressure history in hydrogen/air mixture along r=0 of case 2

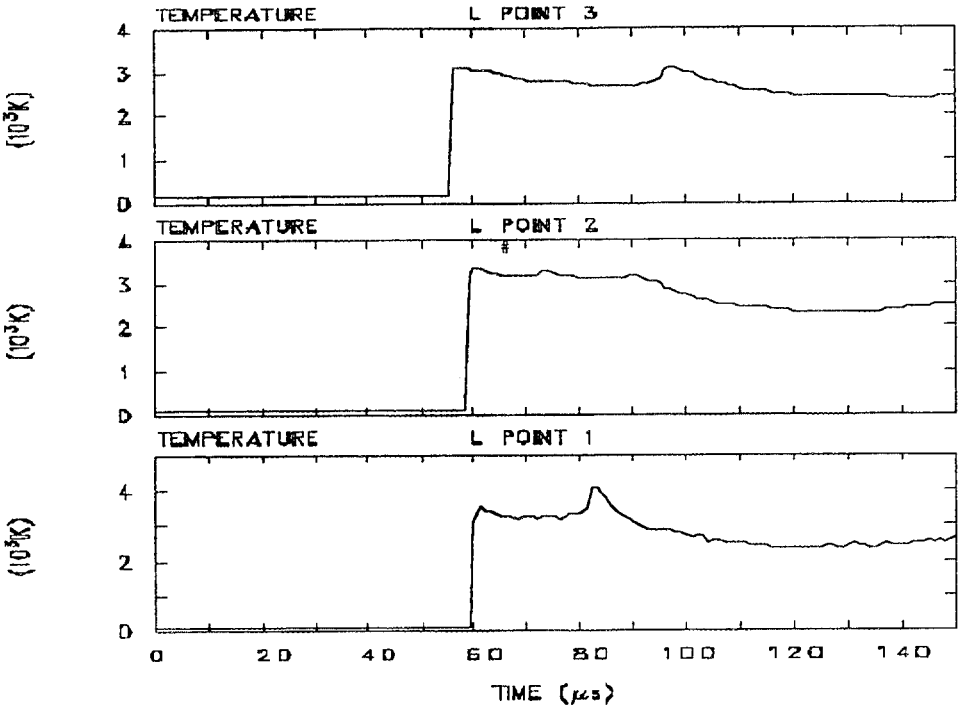

Figure 16(a). Temperature in hydrogen/air mixture near the vacuum tube wall of case 2

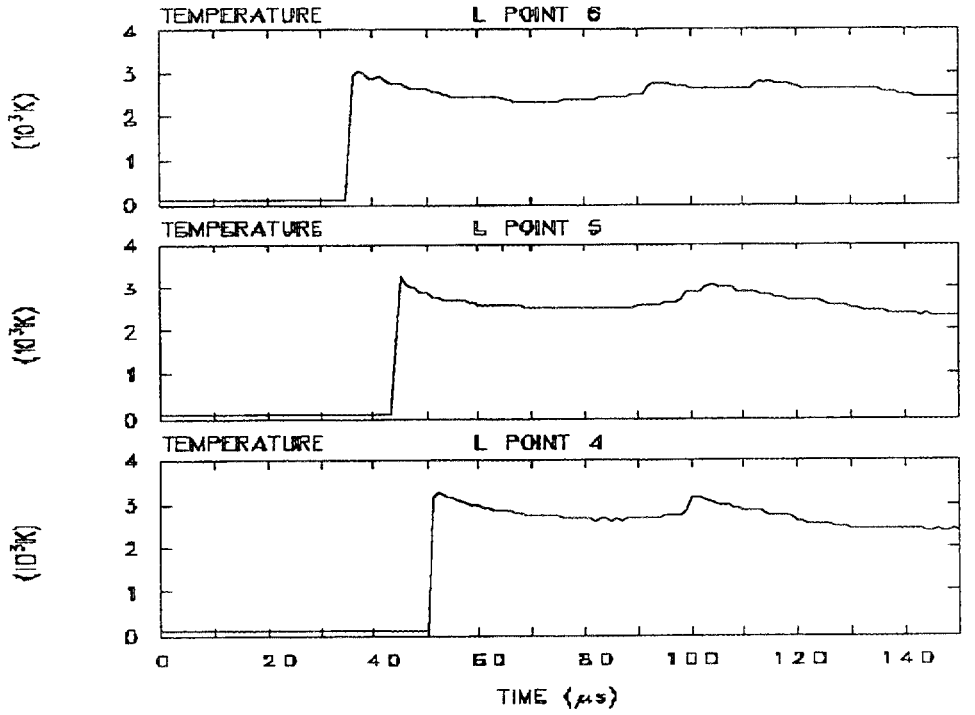

Figure 16(b). Temperature in hydrogen/air mixture near the vacuum tube wall of case 2

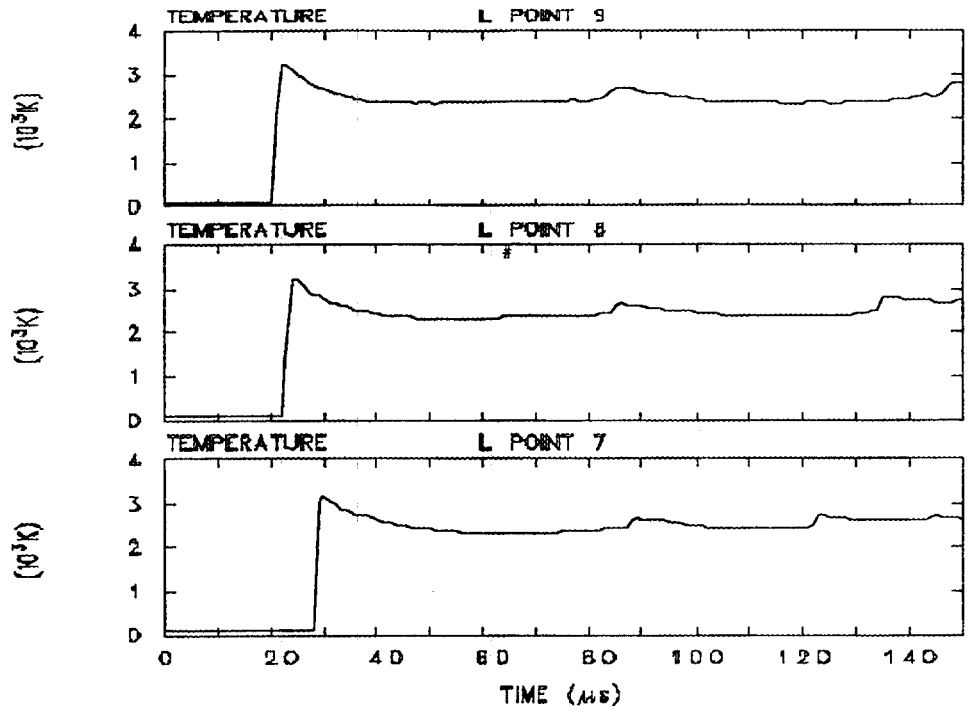

Figure 16(c). Temperature in hydrogen/air mixture near the vacuum tube wall of case 2

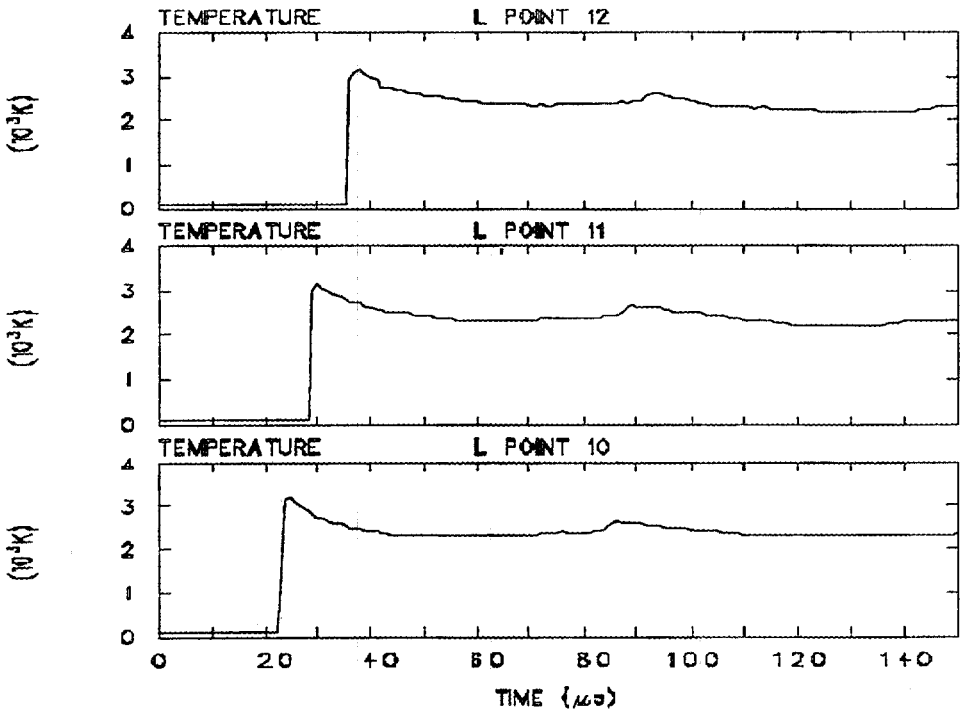

Figure 16(d). Temperature in hydrogen/air mixture near the vacuum tube wall of case 2

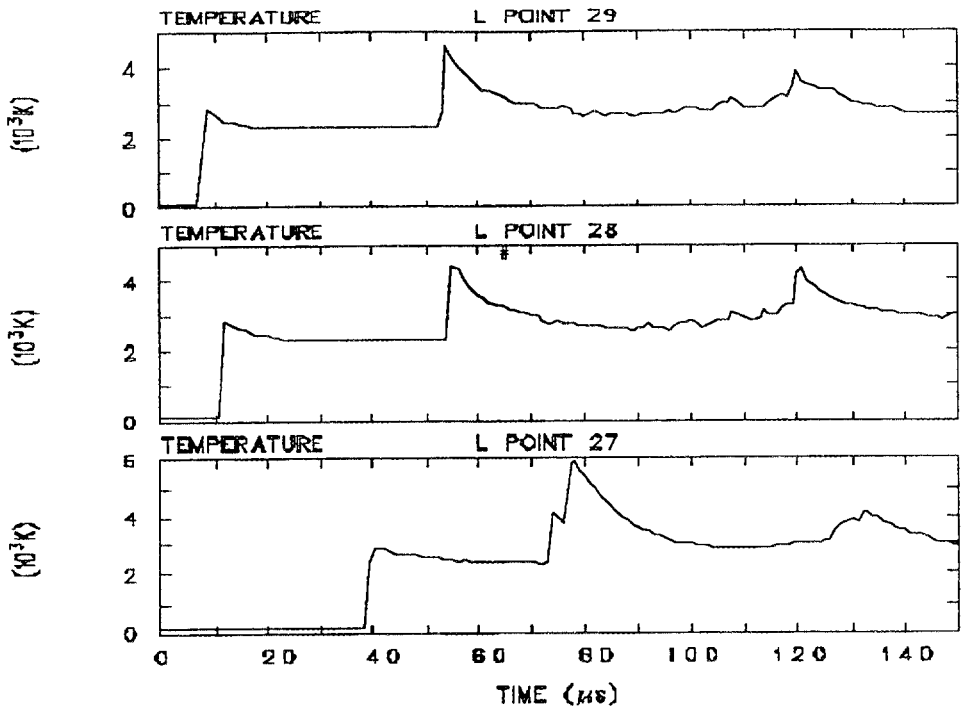

Figure 17. Temperature history in hydrogen/air mixture along r=0 of case 2

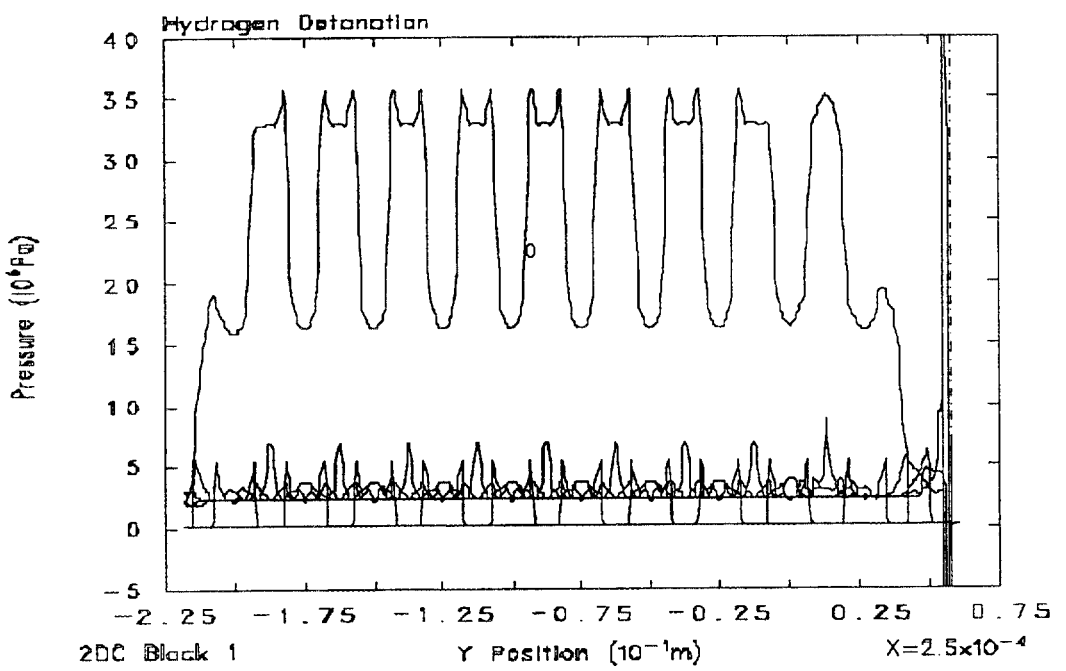

Figure 18(a). Pressure profile along r=0 line from 0 to 18μsec with 3μsec time interval for case 3

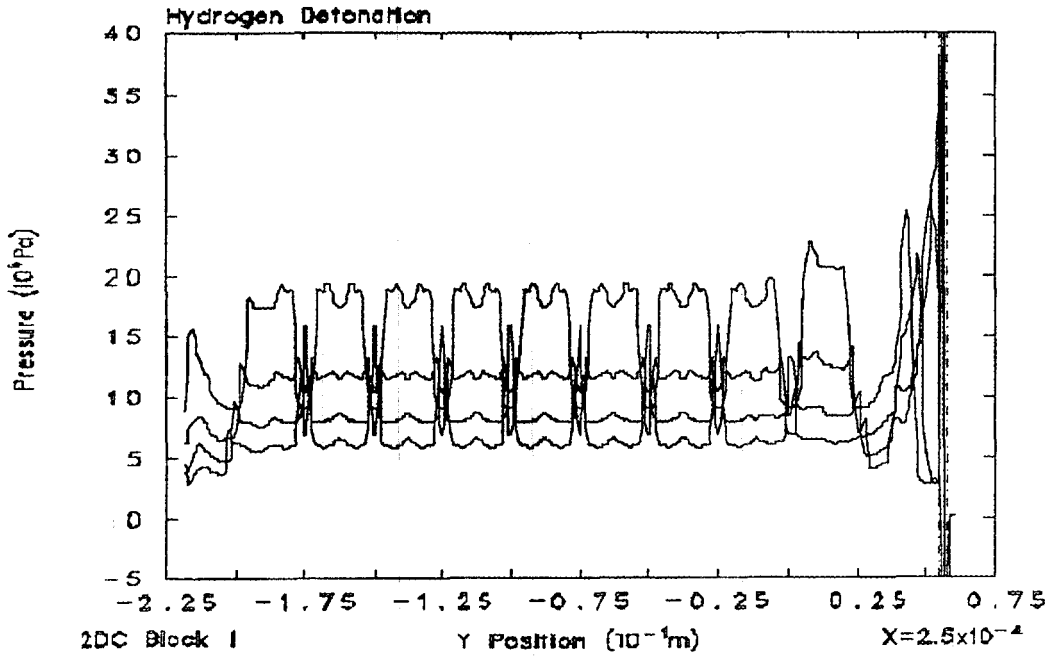

Figure 18(b). Pressure profile along r=0 line from 19 to 22μsec with 1μsec time interval for case 3

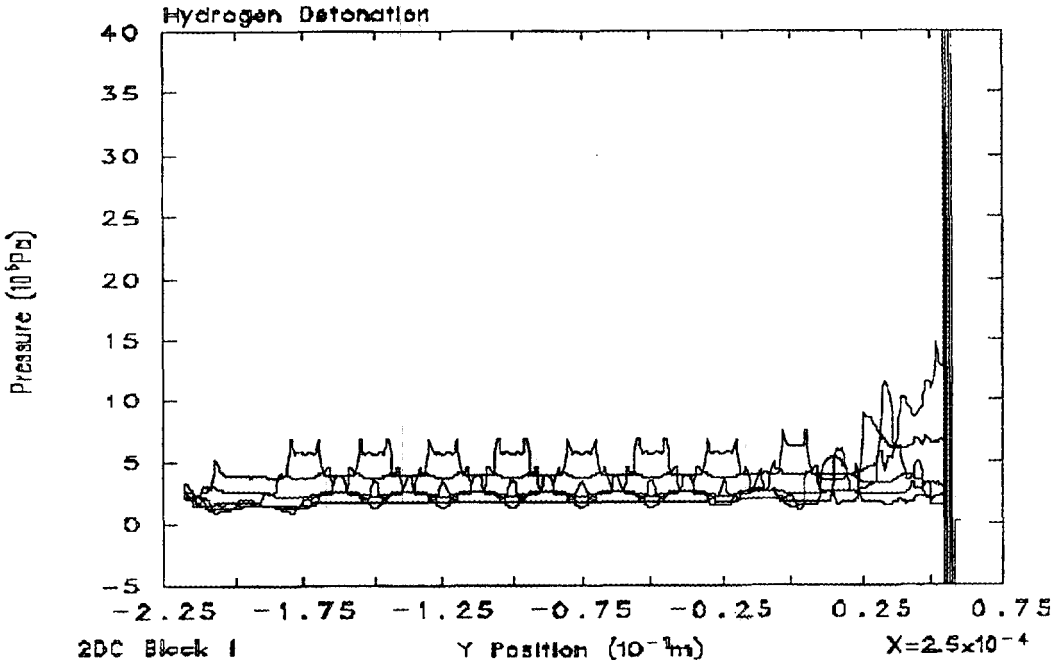

Figure 18(c). Pressure profile along r=0 line from 23 to 39μsec with 3μsec time interval for case 3

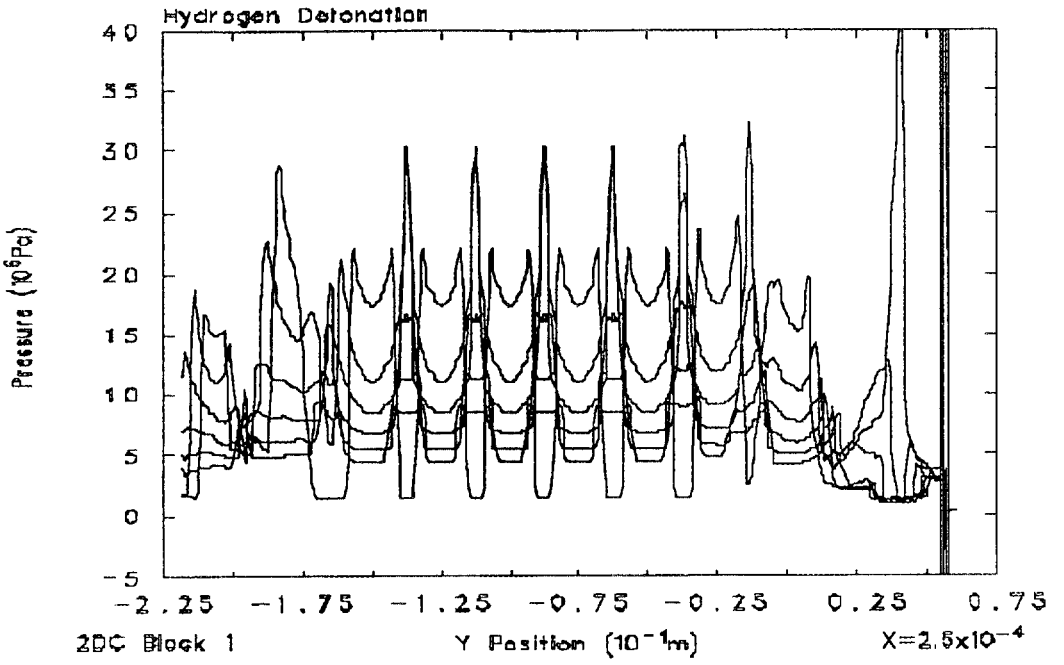

Figure 18(d). Pressure profile along r=0 line from 40 to 46μsec with 1μsec time interval for case 3

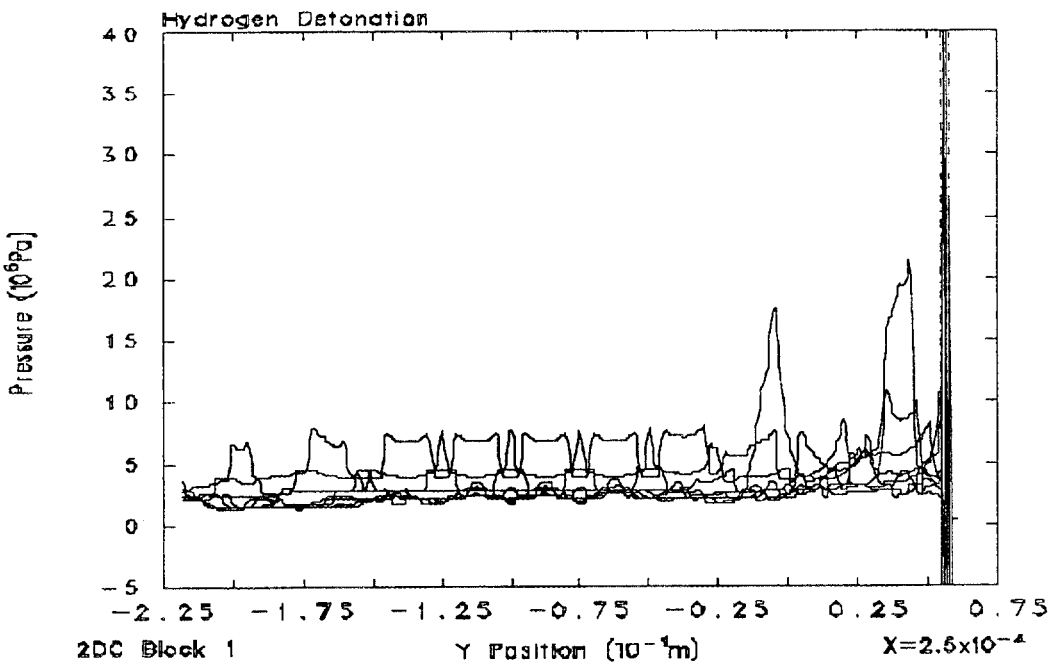

Figure 18(e). Pressure profile along r=0 line from 47 to 70μsec with 3μsec time interval for case 3

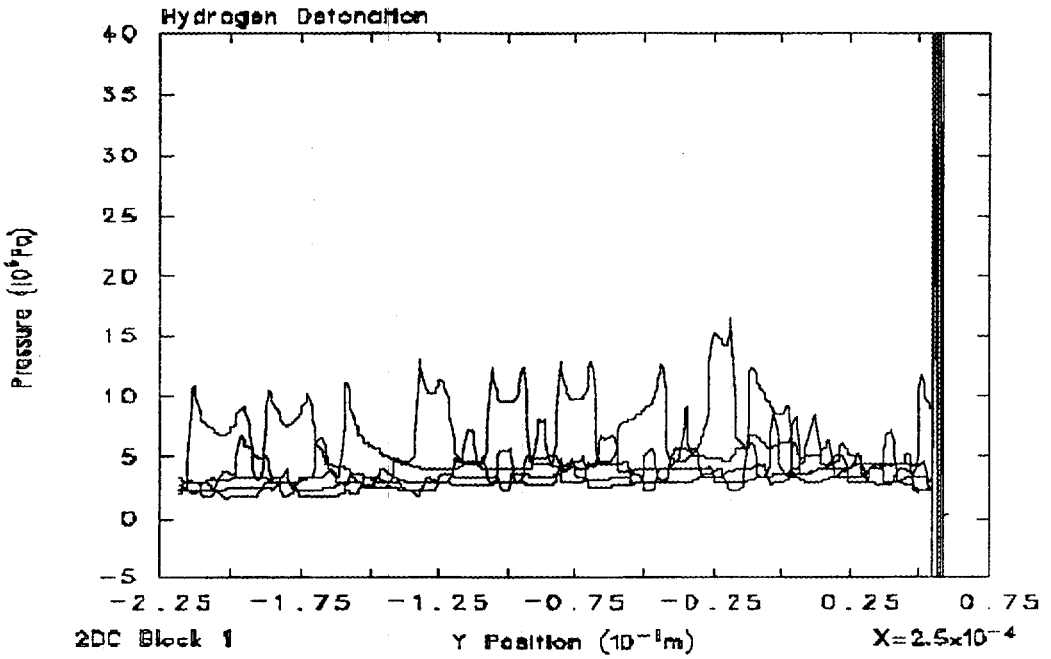

Figure 18(f). Pressure profile along r=0 line from 71 to 86μsec with 3μsec time interval for case 3

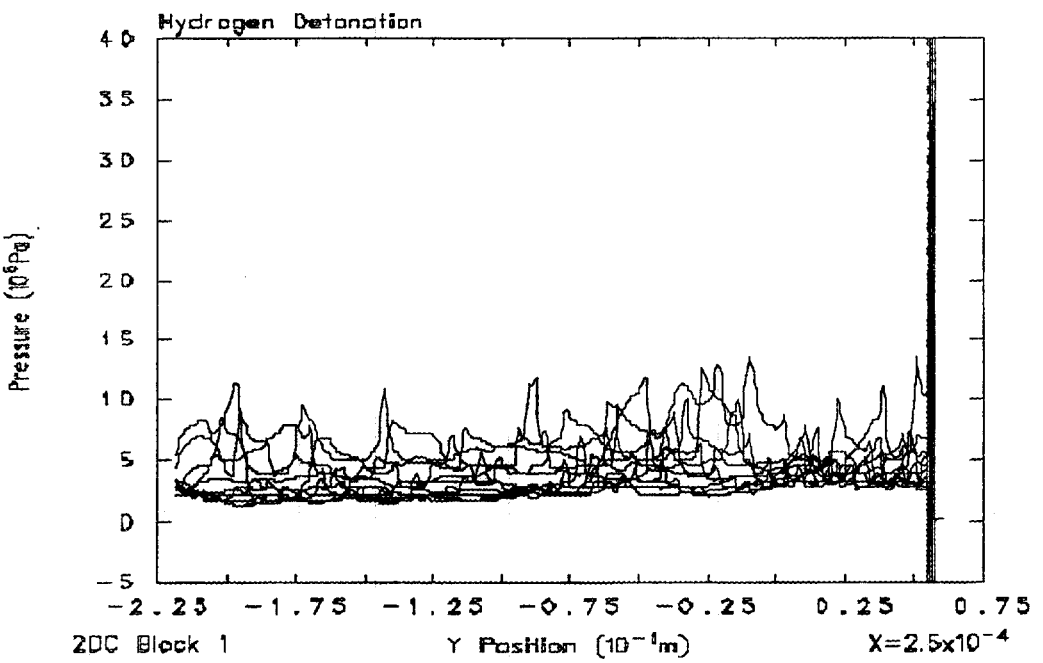

Figure 18(g). Pressure profile along r=0 line from 87 to 119μsec with 3μsec time interval for case 3

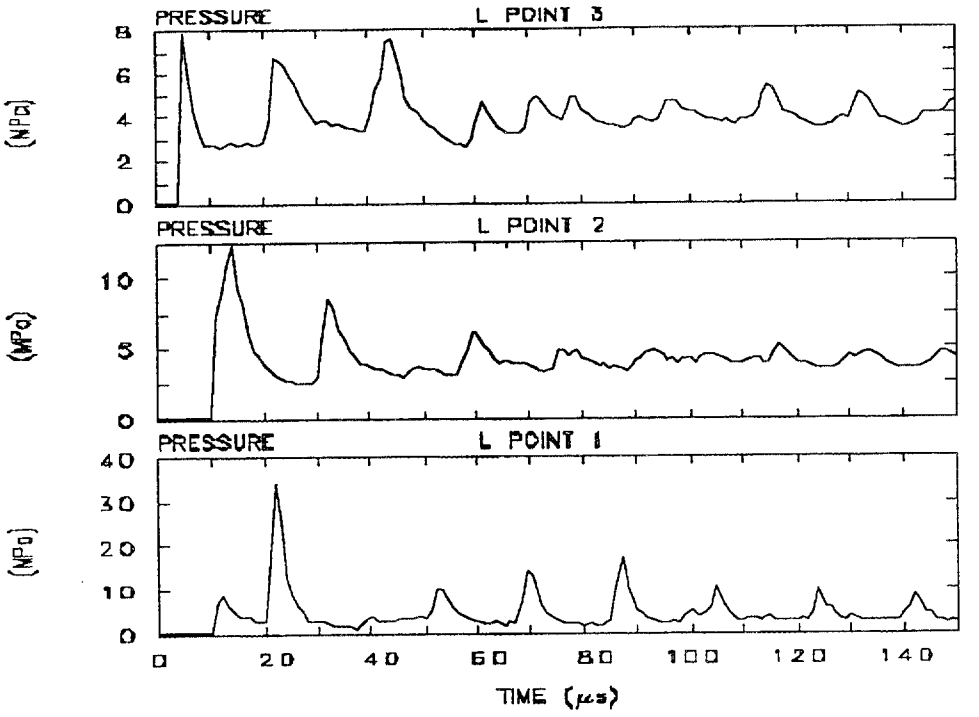

Figure 19(a). Pressure history in hydrogen/air mixture near the vacuum tube wall of case 3

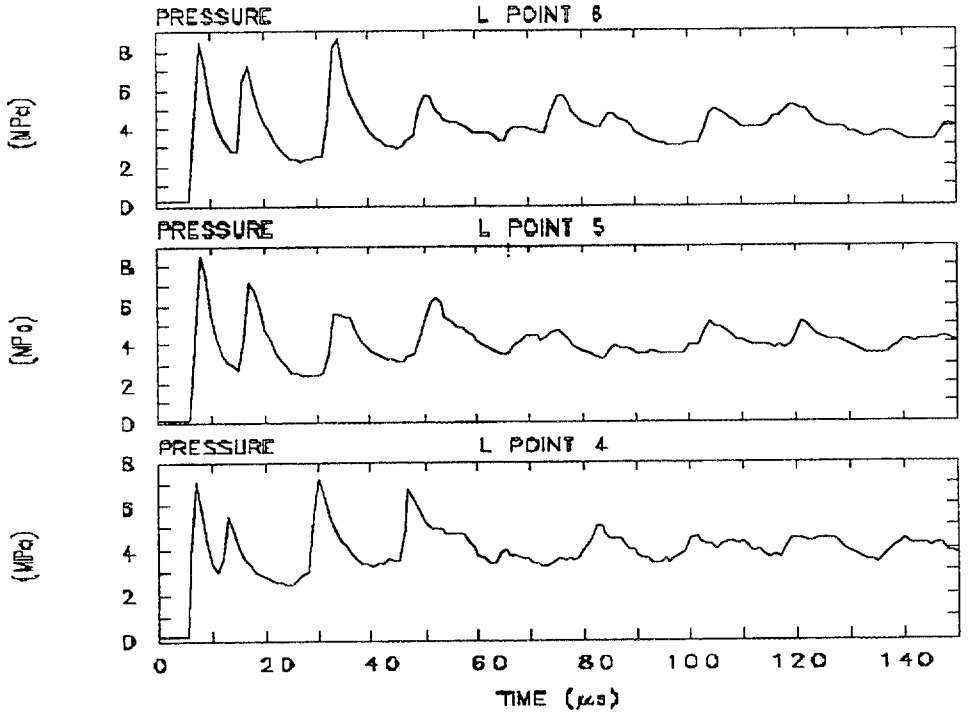

Figure 19(b). Pressure history in hydrogen/air mixture near the vacuum tube wall of case 3

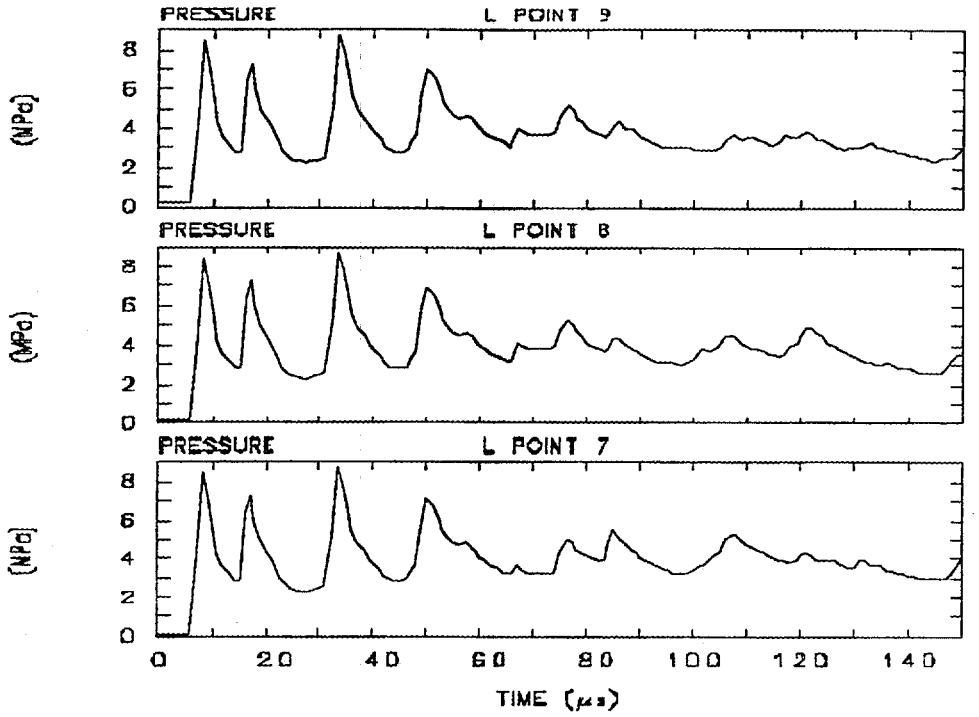

Figure 19(c). Pressure history in hydrogen/air mixture near the vacuum tube wall of case 3

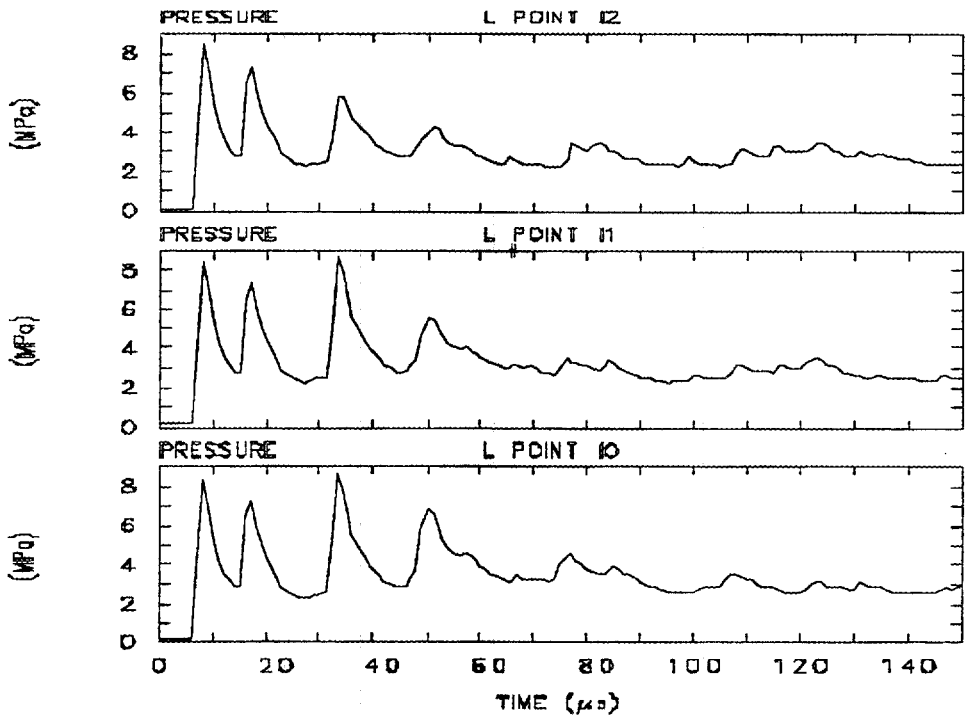

Figure 19(d). Pressure history in hydrogen/air mixture near the vacuum tube wall of case 3

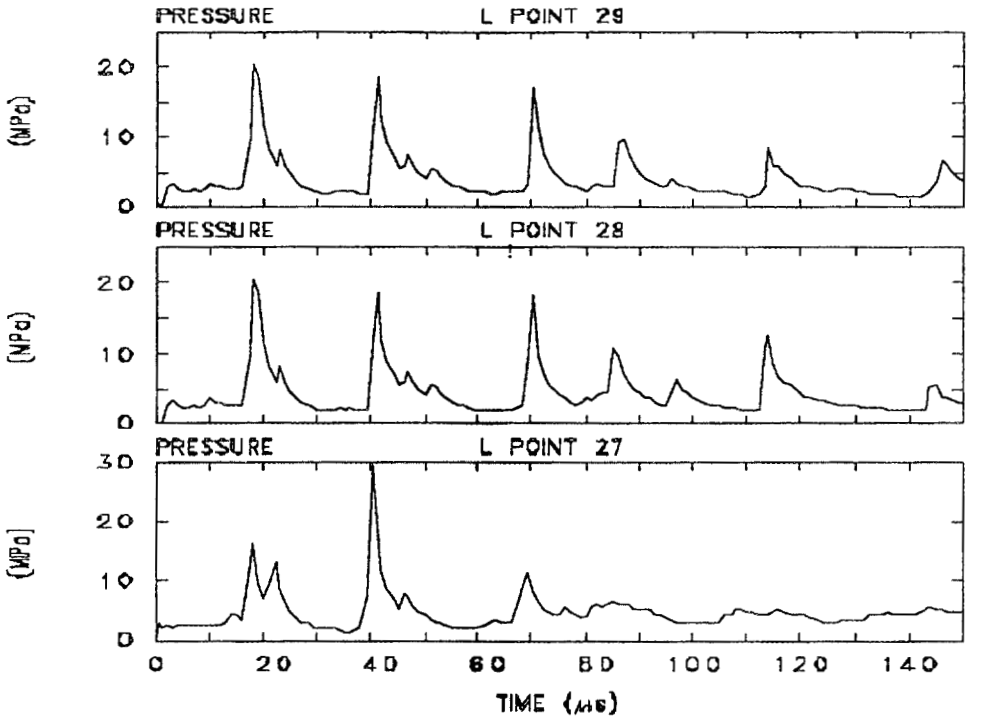

Figure 20. Pressure history in hydrogen/air mixture along r=0 of case 3

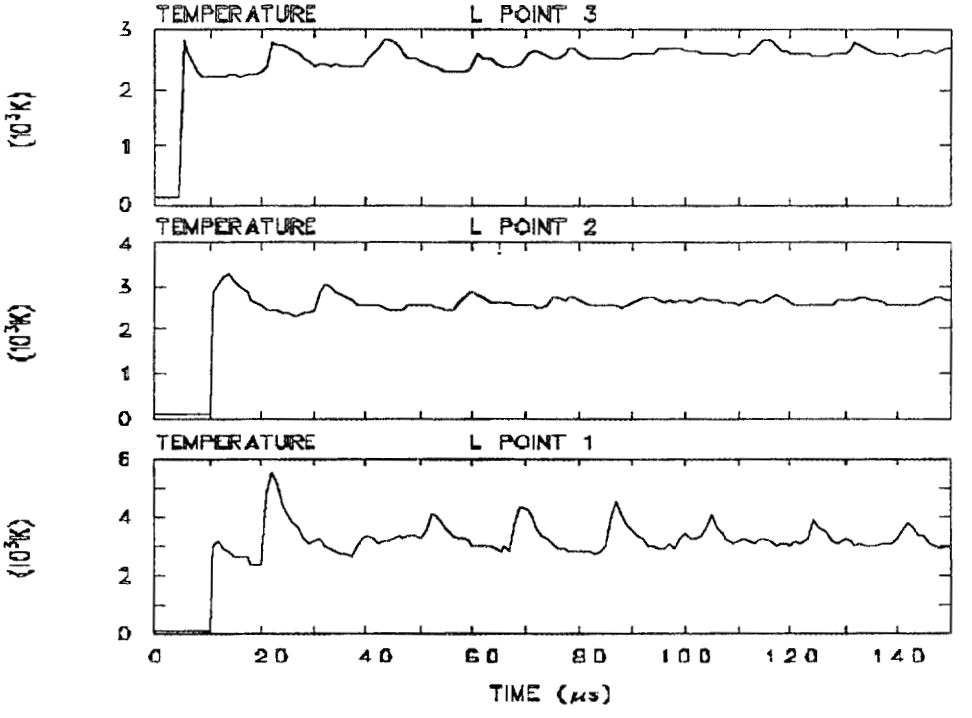

Figure 21(a). Temperature in hydrogen/air mixture near the vacuum tube wall of case 3

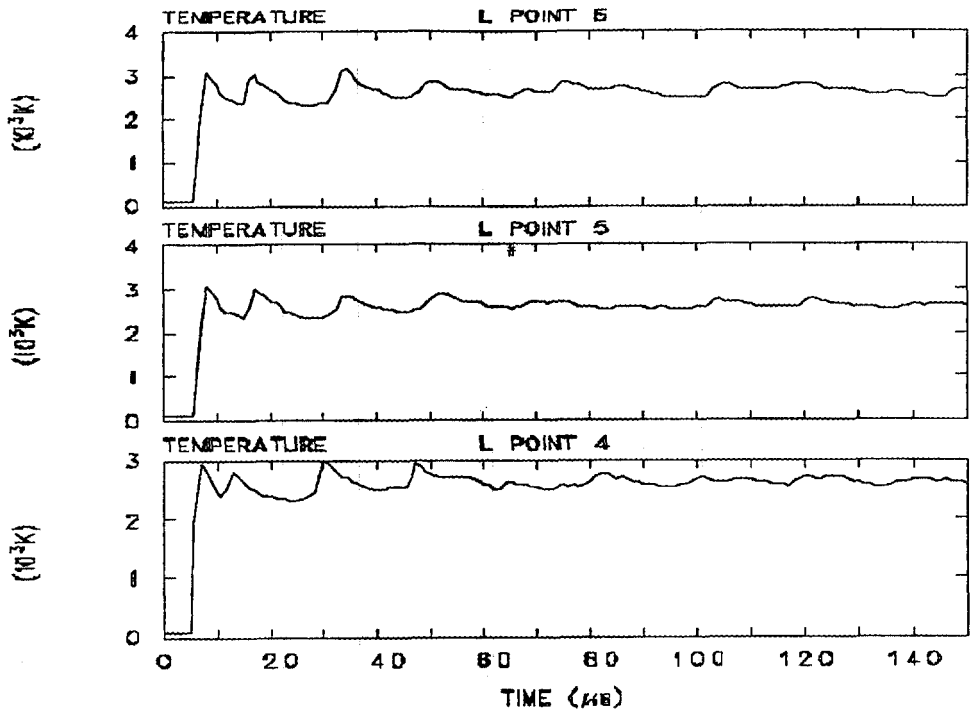

Figure 21(b). Temperature in hydrogen/air mixture near the vacuum tube wall of case 3

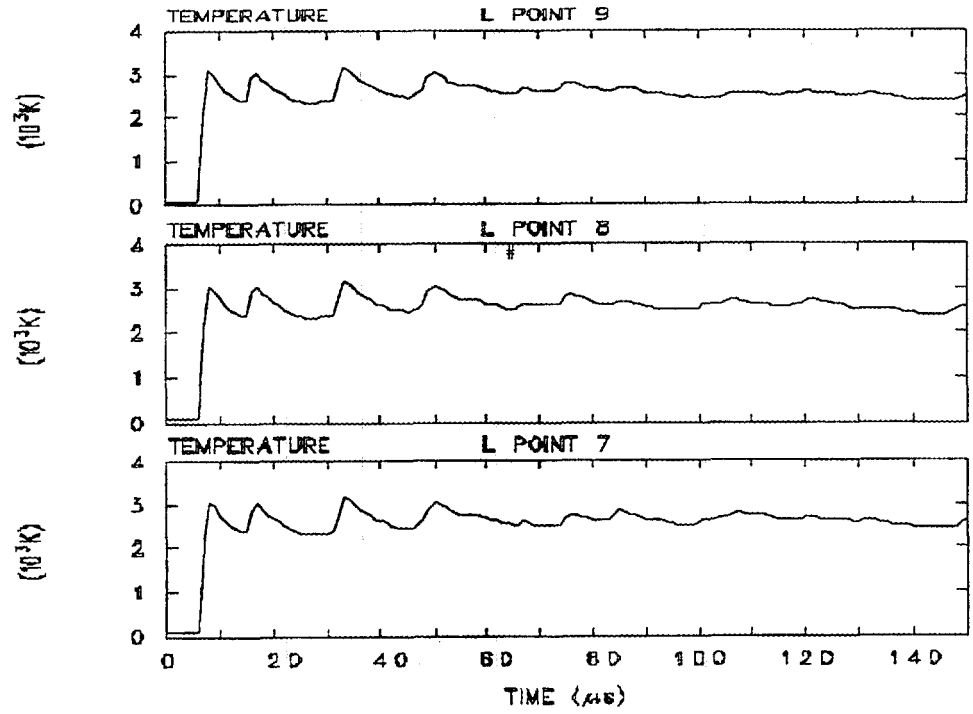

Figure 21(c). Temperature in hydrogen/air mixture near the vacuum tube wall of case 3

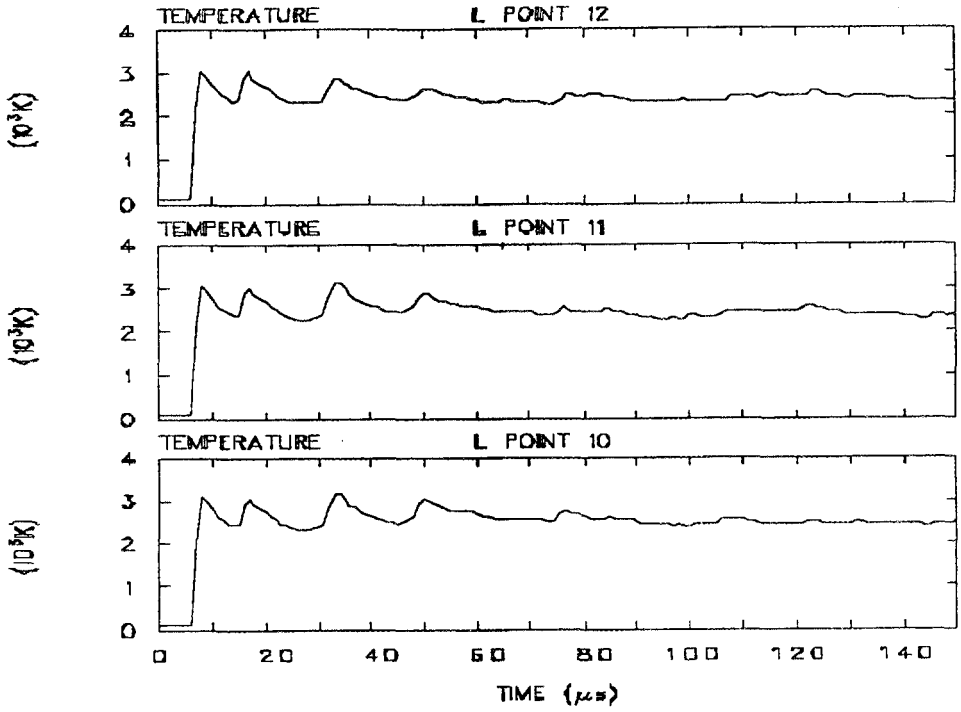

Figure 21(d). Temperature in hydrogen/air mixture near the vacuum tube wall of case 3

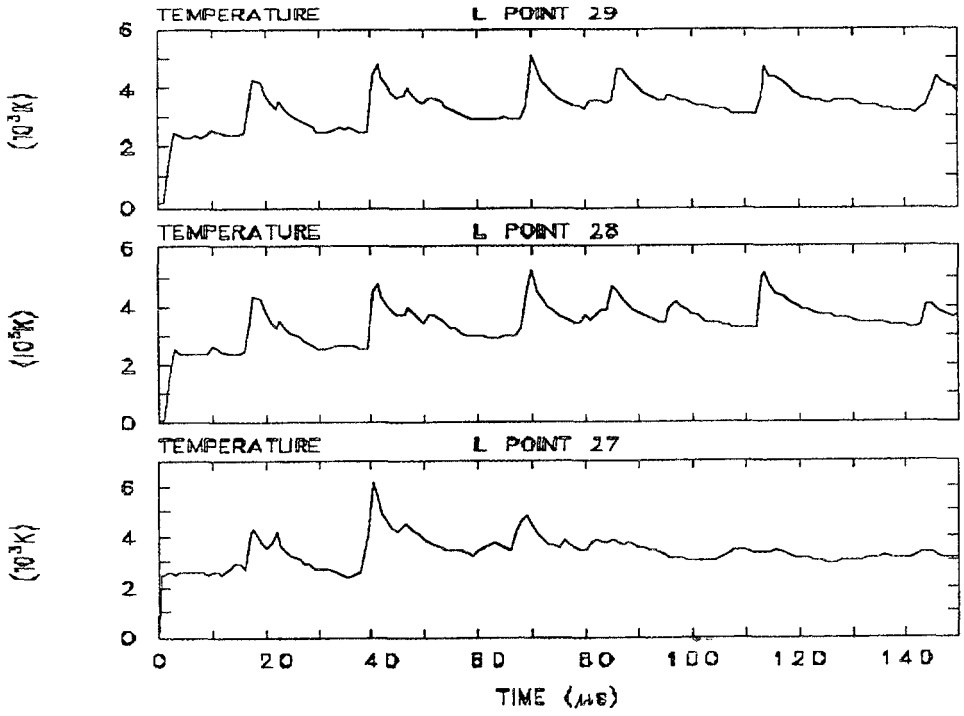

Figure 22. Temperature history in hydrogen/air mixture along r=0 of case 3

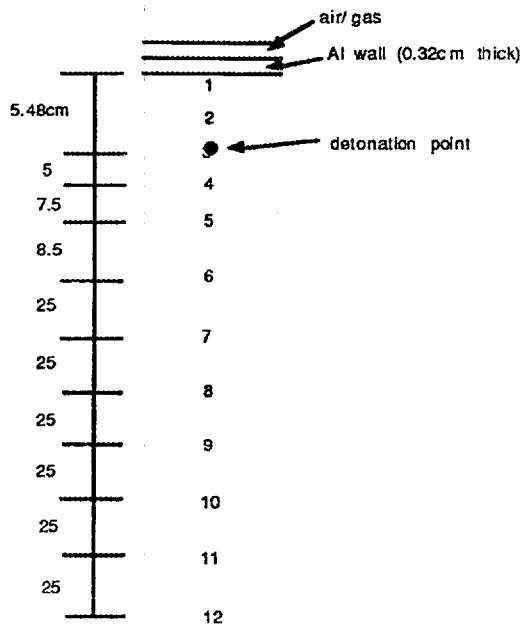

Figure 23. Tracer points modeled in 1-D simulations of case 1

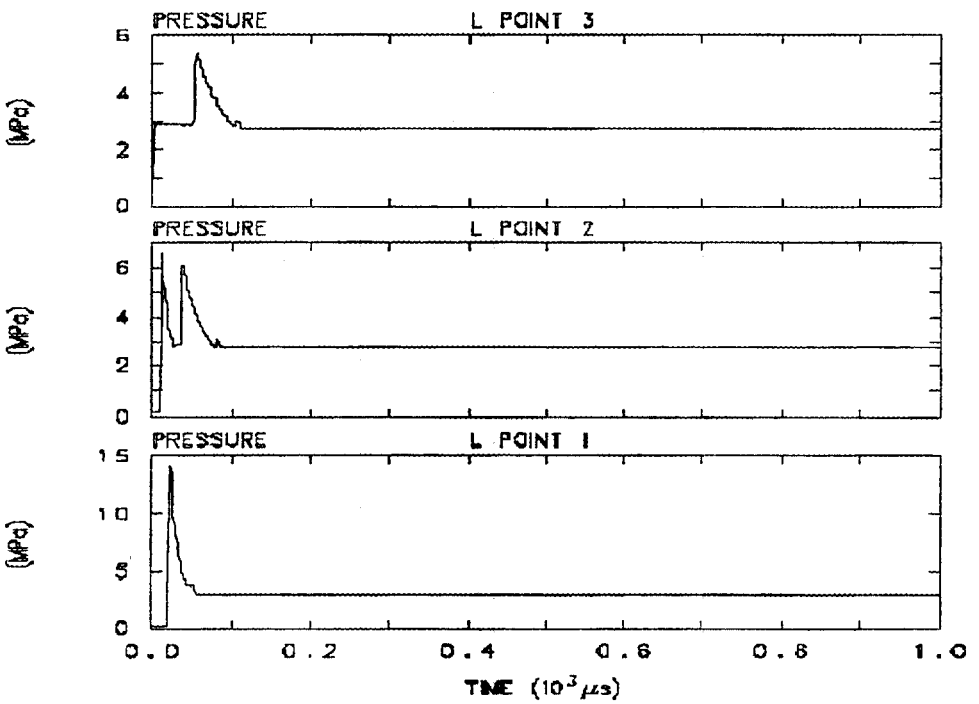

Figure 24(a). Pressure history in hydrogen/air mixture of 1-D simulations

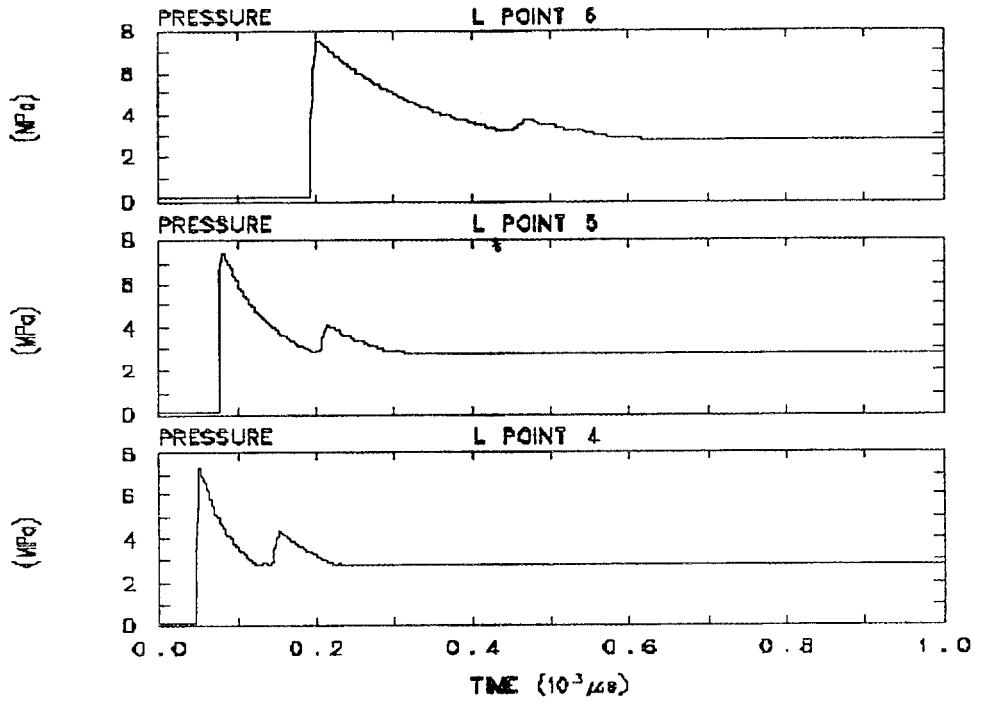

Figure 24(b). Pressure history in hydrogen/air mixture of 1-D simulations

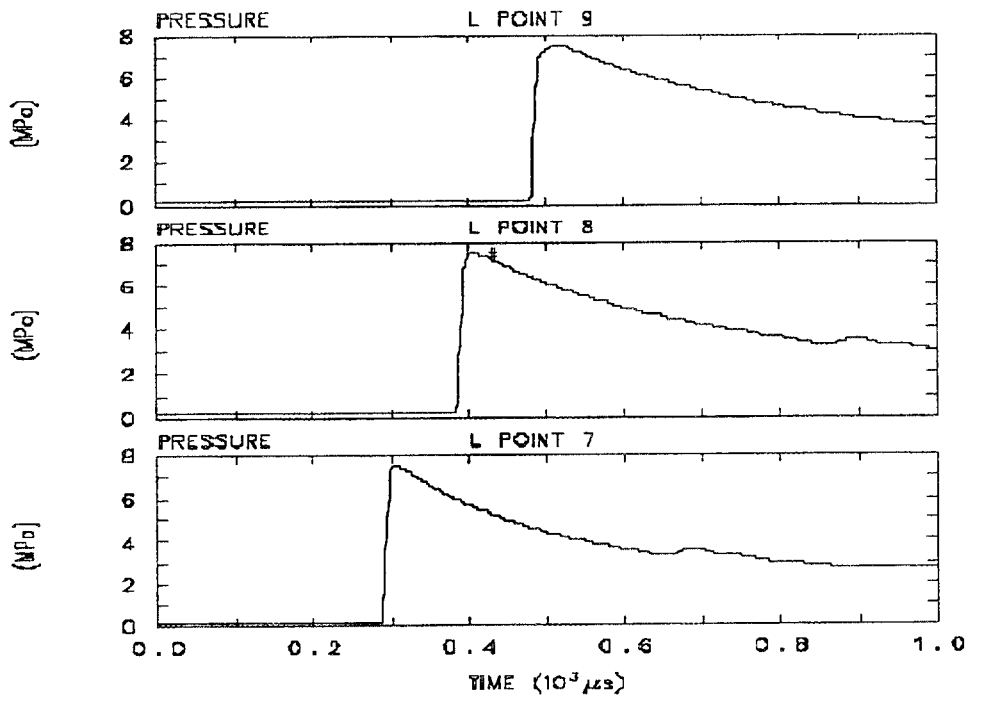

Figure 24(c). Pressure history in hydrogen/air mixture of 1-D simulations

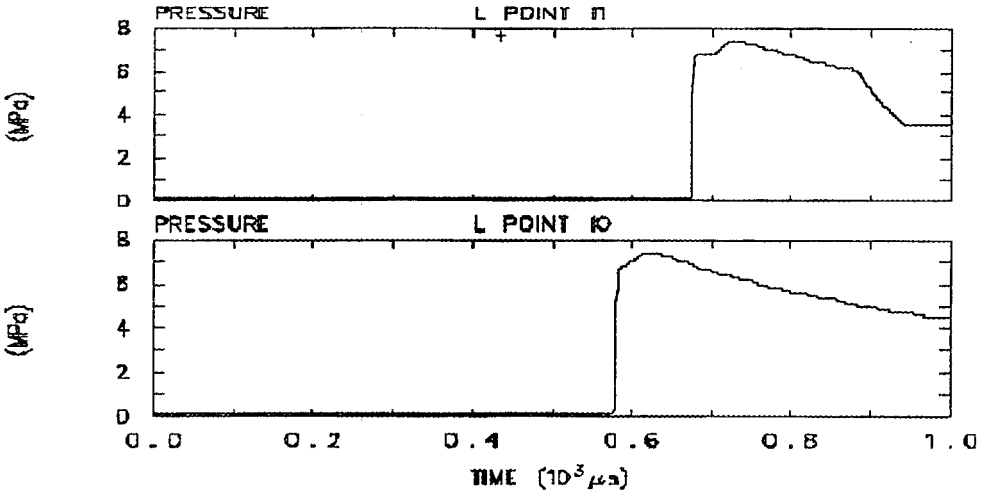

Figure 24(d). Pressure history in hydrogen/air mixture of 1-D simulations

Internal Distrubution List:

1. S. J. Chang
2. D. H. Cook
3. W. G. Craddick
4. E. C. Fox
5. J. D. Freels
6. C. R. Hyman
7. S. H. Kim (3 copies)
8. A. T. Lucas
9. D. L. Selby
10. R. P. Taleyarkhan (3 copies)
11. A. T. Lucas
12. ORNL Patent Section
13. Central Research Library
14. Laboratory Records Department